ELECTRONIC SUPPLIMENTRY INFORMATION

A selective hydrolytic and restructuring approach through a Schiff base design on a coumarin platform for "turn-on" fluorogenic sensing of Zn^{2+}†

Abha Pandey,[a] Sharad Kumar Asthana,[a] Anand Prakash,[b] Jagat Kumar Roy,[b] Ida Tiwari,[a] and K. K. Upadhyay[a]*

Department of Chemistry (Centre of Advanced Study), Institute of Science, Banaras Hindu University, Varanasi, Uttar Pradesh, India-221005,

**Corresponding author: Tel: +91 542 670 2488*

***E-mail:** drkaushalbhu@ yahoo.co.in; kku@bhu.ac.in, Tel: +91-542-6702488*

[b]*Department of Zoology, Institute of Science, Banaras Hindu University, Varanasi-221005, Varanasi, Uttar Pradesh, India-221005*

Table of Contents

EXPERIMENTAL SECTION

1.1 Instrumentation:

The IR Spectra were recorded on JASCO-FTIR Spectrophotometer while ^{1}H NMR and ^{13}C NMR spectra were recorded on JEOL AL 500 FT NMR Spectrometer. Mass spectrometric analysis was carried out on a Brukar Compass data analysis spectrometer. Electronic spectra were recorded at room temperature (298 K) on a UV-1700 pharmaspec spectrophotometer with quartz cuvette (path length=1 cm). Emission spectra were recorded on JY HORIBA Fluorescence spectrophotometer.

1.2 Materials and methods:

All reagents for synthesis were purchased from Sigma-Aldrich and were used without any further purification. All titration experiments were carried at room temperature. All the cations were used as their chloride salts. The ^{1}H NMR spectra were recorded by using tetramethylsilane (TMS) as an internal reference standard.

1.3 Cell culture

SiHa and HeLa cells were used in this study. Cells were maintained in the Dulbecco's modified Eagle's medium (DMEM, HiMedia), 10% fetal bovine serum (Invitrogen), and 1X antibiotic cocktail (HiMedia) and incubated in a 5% CO2 incubator at 37˚C. Cells were washed with I x PBS and trypsinized before seeding for experimental setup. Cells were seeded onto gelatin-coated 6-well plates and cultured for 24 h.

1.4 Cellular imaging methodology

Fluorescent property of the compound CMD with or without presence of Zn^{++} was studied on the SiHa cell line. Overnight grown more than 60 % confluent cells were used for experiment. cells were seeded in glass cover slip added 6- well plate and allowed to grow in complete media which was prepared in DMEM with 10% FBS and 1X antibiotic cocktail. Overnight grown cells were treated with 10μM and 20μM CMD without Zn^{2+} and in the presence of Zn^{2+}(5 times higher than CMD concentration) incubated for 6h on. Cells were washed with 1X PBS and fixed with 4% PFA for 15 min followed by 3 times 0.1% PBST washing, further stained with DAPI for 10 min and again washed with 0.1% PBST. Unstained DAPI were removed by washing with 0.1% PBST, 3 times further cells were mount in DABCO and imaging under confocal microscope and analyzed by LSM510-Meta software.

1.5 Cell viability experiment:

MTT assay: To check the cell viability of cells in the presence of CMD MTT (3-(4, 5-dimethylthiazol-2-yl)-2,5-diphenyl-2H-tetrazolium bromide) colorimetric assay was done. Hela cells were seeded (1×10^4 cells/well) in a 96-well plate in 100 µl complete media and incubated for 24 h at 37°C and 5% CO_2. After 24 h of incubation culture were replaced with fresh media containing CMD with varying concentrations for 24 h or 48 h. After required period of incubation of compound, cells were washed with 1X PBS and then 10µl of MTT solution (HiMedia) (5 mg ml-1 stock prepared in 1X PBS) in 100 µl of medium were added in culture and incubated for 3h at 37°C. After sometime formazan crystals were formed which in the presence of dimethyl sulfoxide (DMSO) dissolved and develops color in 10 to 15 minutes that was measured by a micro plate reader (Bio-RAD 680, USA) at 570 nm.

1.6 Determination of Quantum yield (Φ)

For measurement of the quantum yields of various species**,** we recorded the absorbance of the compounds in aqueous medium. The emission spectra were recorded using the maximal excitation wavelengths, and the integrated areas of the fluorescence-corrected spectra were measured. The quantum yields were then calculated by comparison with quinine sulphate (0.1M H_2SO_4, Φs = 0.58 in water) as reference using the following equation:

$$\boldsymbol{\Phi x = \Phi s \times (Ix/Is) \times (As/Ax) \times (nx/ns)2}$$

Where, x & s indicate the unknown and standard solution respectively, Φ is the quantum yield, I is the integrated area under the fluorescence spectra, A is the absorbance and n is the refractive index of the solvent.

1.7 X-ray diffraction studies:

The single crystal X-ray diffraction measurements were carried out on an Oxford Diffraction Xcalibur system with a Ruby CCD detector as well as on a Bruker SMART APEX CCD diffractometer using graphite-monochromated MoKa radiation (k = 0.71073 Å). All the determinations of unit cell and intensity data were performed with graphite monochromated Mo-Kα radiation (λ=0.71073 A°). Data for the ligands and metal complex were collected at room temperature liquid nitrogen temperature. The structures were solved by direct methods, using Fourier techniques and refined by full-matrix least-squares on F2 using the SHELXTL-97 program package.[S1] Crystal data and details of the structure determination for **CMD, NSA** and **CM-Zn-CM'** are summarized in Table S1. CCDC no. of **CMD** and **CM-Zn-CM'** are CCDC 1588901 and 1836451 respectively which contain the supplementary crystallographic data for this paper. These data can be obtained free of charge from the Cambridge Crystallographic Data Centre via http://www.ccdc.cam.ac.uk/cgi-bin/catreq.cgi.

References: S1. (a) G. M. Sheldrick, SHELXL-97, Program for X-ray Crystal Structure Refinement, Göttingen University, Göttingen, Germany, 1997; (b) G. M. Sheldrick, SHELXS-97, Program for X-ray Crystal Structure Solution, Göttingen University, Göttingen, Germany, 1997.

TABLE S1: Crystal data of CMD, NSA and CM-Zn-CM'

Identification code	**CMD**	**NSA**	**CM-Zn-CM'**
CCDC No.	**CCDC 1588901**	**CCDC 1856059**	**CCDC 1836451**
Empirical formula	**$C_{22}H_{23}N_3O_4$**	**C_{11} H_{15} N_2 O**	**C_{53} H_{60} N_6 O_{18} S_4 Zn_2**
Formula weight	393.43	191.25	1328.05
Temperature	100(2)K	100(2) K	273(2)K
Crystal system	Monoclinic	Triclinic	Monoclinic
space group	P2(1)/c	P-1	P 21/n
Unit cell dimensions	a= 10.2228(5)Å , alpha=90 (2)deg. b= 10.0210(5)Å, beta=95.874(2)deg. c= 18.7682(10) Å, gamma=90 deg.	a = 6.8677(10) A alpha = 78.996(5) deg. b = 8.2475(12) A beta = 69.498(4) deg. c = 9.6475(14) A gamma = 83.187(4) deg.	a= 18.1235(8), alpha =90 deg. b= 16.7124(7), beta= 102.8000(10) deg. c=20.6274(9), gamma = 90 deg.
Volume	1912.57(17)Å^3	501.63(13) A^3	6092.5(5) Å^3
Z	4	2	4
Density (calculated)	1.366 mg m^{-3}	1.266 Mg/m^3	1.448
Absorption coefficient	0.095 mm^-1	0.083 mm^-1	0.998 mm^-1
F(000)	832	206	2752
Crystal size	0.21 x 0.18 x 0.14 mm	0.19 x 0.16 x 0.11 mm	0.28 x 0.20 x 0.15 mm
Crystal color and habit	Orange, Block	Yellow, Block shape	Yellow, Block
Diffractometer	'Bruker APEX-II CCD'	'Bruker APEX-II CCD'	'Bruker APEX-II CCD'
Theta range for data collection	2.807 to 28.354 deg.	3.118 to 28.372 deg.	2.363 to 28.477 deg
Limiting indices	-13<=h<=13, -13<=k<=13, -24<=l<=25	-9<=h<=9, -11<=k<=11, -12<=l<=12	-24<=h<=24, -22<=k<=22, -27<=l<=27
Reflections collected / unique	23087/ 4775 [R(int) = 0.0760]	7764 / 2497 [R(int) = 0.0741]	91447 / 15293 [R(int) = 0.1181]
Completeness to theta = 25.00	99.9 %	99.6 %	99.9 %
Refinement method	Full-matrix least-squares on F^2	Full-matrix least-squares on F^2	Full-matrix least-squares on F^2
Data / restraints / parameters	4775 / 0 / 290	2497 / 0 / 130	15293 / 66 / 814
Goodness-of-fit on F^2	0.959	1.042	1.035
Final R indices [I>2sigma(I)]	R1 = 0.0657, wR2 = 0.1454	R1 = 0.0656, wR2 = 0.1701	R1 = 0.0690, wR2 = 0.1421
R indices (all data)	R1 = 0.1599, wR2 = 0.1874	R1 = 0.0823, wR2 = 0.1881	R1 = 0.1289, wR2 = 0.1626
Largest diff. peak and hole	0.0.241 and -0.292 e.A^-3	0.356 and -0.354 e.A^-3	0.964 and -1.300 e.A^-3

TABLE S2: IMPORTANT BOND LENGTH AND BOND ANGLE FOR THE COMPLEX

Bond angles					Bond angles					Bond distances			
1	O1W	Zn1	O3	99.9(1)	36	Zn2	O2W	H2WB	101.4	1	Zn1	O1W	2.061(3)
2	O1W	Zn1	O10	86.7(1)	37	H2WA		O2W	H2WB				
3	O1W	Zn1	N1	96.0(1)		106.7				2	Zn1	O3	2.043(3)
4	O1W	Zn1	N3	81.2(1)	38	Zn1	O3	C8	132.4(2)				
5	O1W	Zn1	N6	157.8(1)	39	Zn2	O4	C15	132.4(2)	3	Zn1	O10	2.032(3)
6	O3	Zn1	O10	96.6(1)	40	C19	O5	C23	122.3(3)				
7	O3	Zn1	N1	85.2(1)	41	C24	O8	C33	122.4(3)	4	Zn1	N1	2.118(4)
8	O3	Zn1	N3	159.1(1)	42	Zn2	O9	C31	132.6(2)				
9	O3	Zn1	N6	100.9(1)	43	Zn1	O10	C37	127.2(2)	5	Zn1	N3	2.520(3)
10	O10	Zn1	N1	176.5(1)	44	C41	O11	C45	121.9(3)				
11	O10	Zn1	N3	104.3(1)	45	Zn1	N1	N2	115.6(2)	6	Zn1	N6	2.104(3)
12	O10	Zn1	N6	83.2(1)	46	Zn1	N1	C11	128.7(3)				
13	N1	Zn1	N3	73.9(1)	47	N2	N1	C11	114.3(3)	7	Zn2	O2W	2.129(3)
14	N1	Zn1	N6	93.5(1)	48	Zn2	N2	N1	107.2(2)				
15	N3	Zn1	N6	82.1(1)	49	Zn2	N2	C12	105.0(2)	8	Zn2	O4	2.029(3)
16	O2W	Zn2	O4	92.0(1)	50	Zn2	N2	H2N	112.6				
17	O2W	Zn2	O9	89.6(1)	51	N1	N2	C12	110.0(3)	9	Zn2	O9	2.021(3)
18	O2W	Zn2	N2	81.6(1)	52	N1	N2	H2N	111.3				
19	O2W	Zn2	N4	93.4(1)	53	C12	N2	H2N	110.5	10	Zn2	N2	2.351(3)
20	O2W	Zn2	N5	169.8(1)	54	Zn1	N3	N4	112.2(2)				
21	O4	Zn2	O9	104.7(1)	55	Zn1	N3	C12	98.5(2)	11	Zn2	N4	2.142(3)
22	O4	Zn2	N2	158.9(1)	56	Zn1	N3	H3N	118(2)				
23	O4	Zn2	N4	85.4(1)	57	N4	N3	C12	108.3(3)	12	Zn2	N5	2.139(3)
24	O4	Zn2	N5	97.9(1)	58	N4	N3	H3N	111(3)				
25	O9	Zn2	N2	95.4(1)	59	C12	N3	H3N	108(3)				

Figure S1: IR spectrum of **4-methyl-7-hydroxycoumarinol**

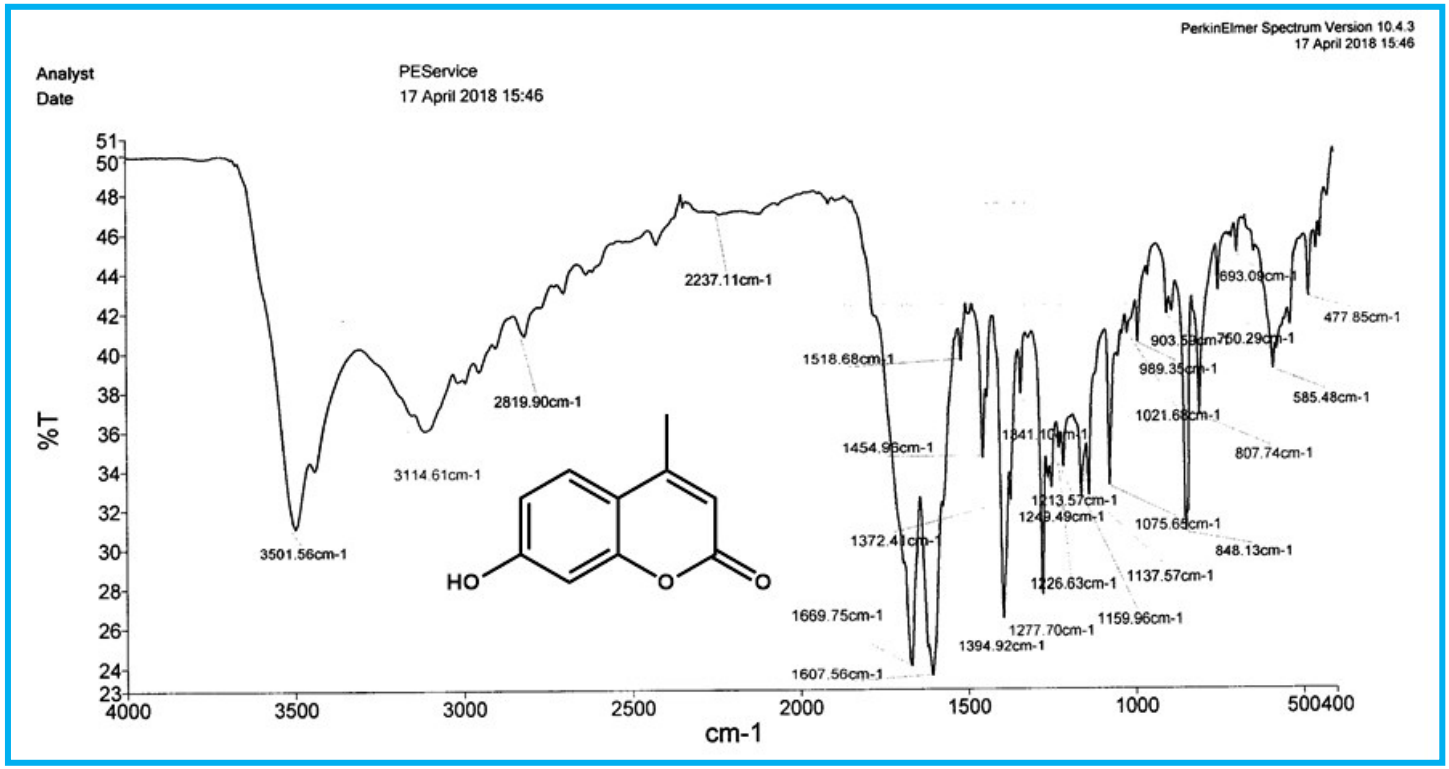

Figure S2: IR spectrum of **ACM**

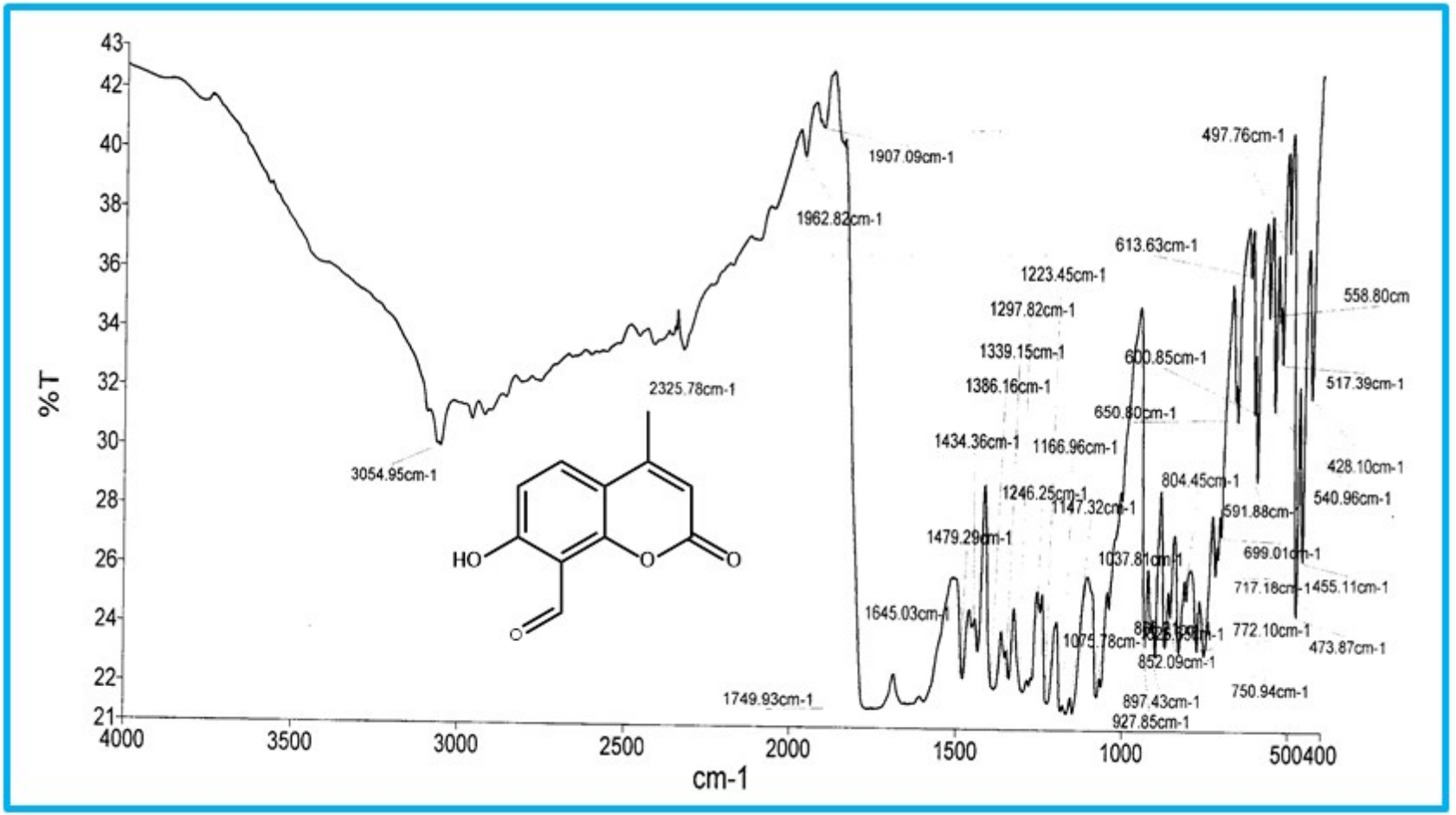

Figure S3: ^{1}H NMR spectrum of **ACM** (in $CDCl_3$)

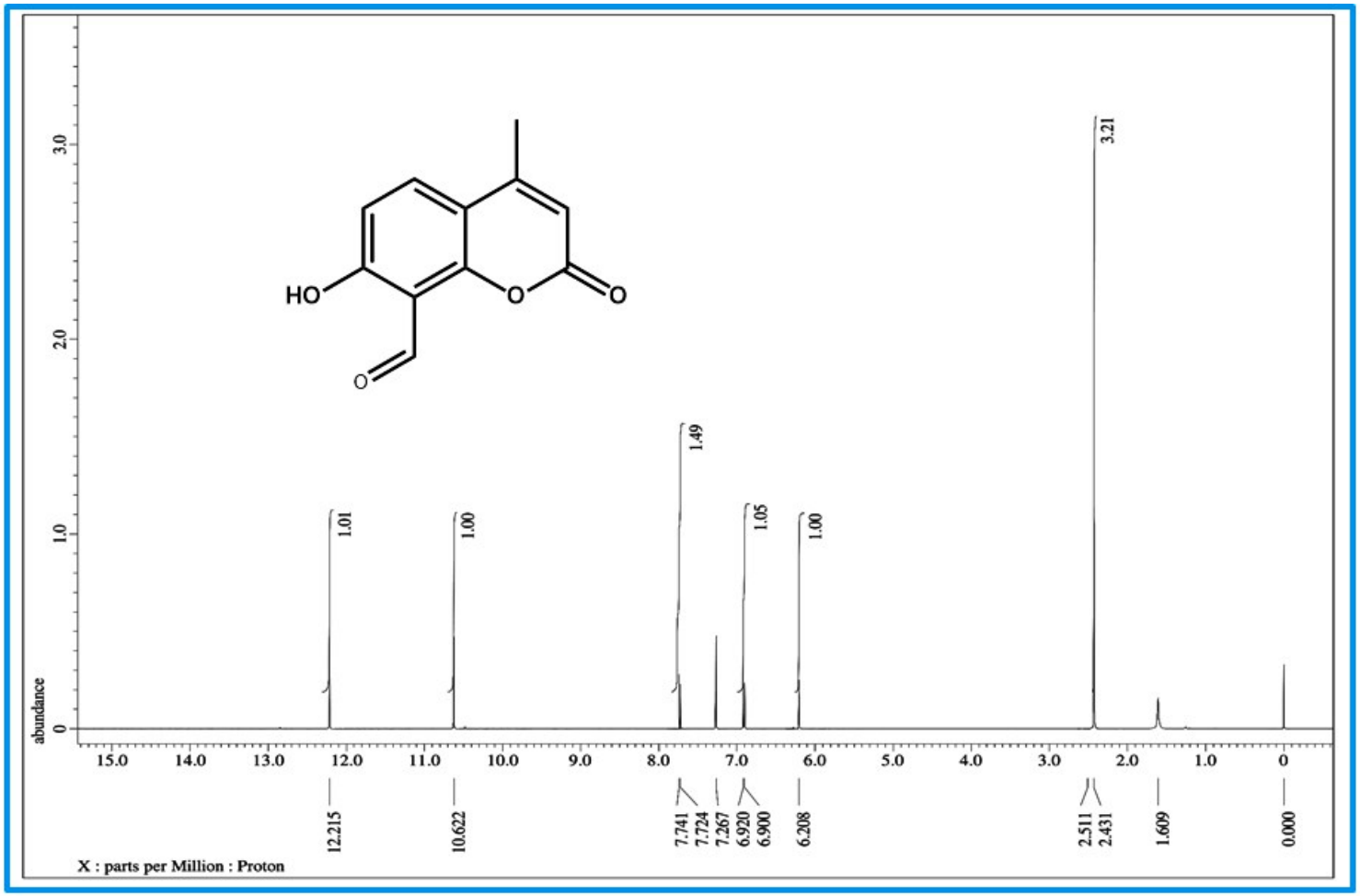

Figure S4: IR spectrum of **ACM-Hz**

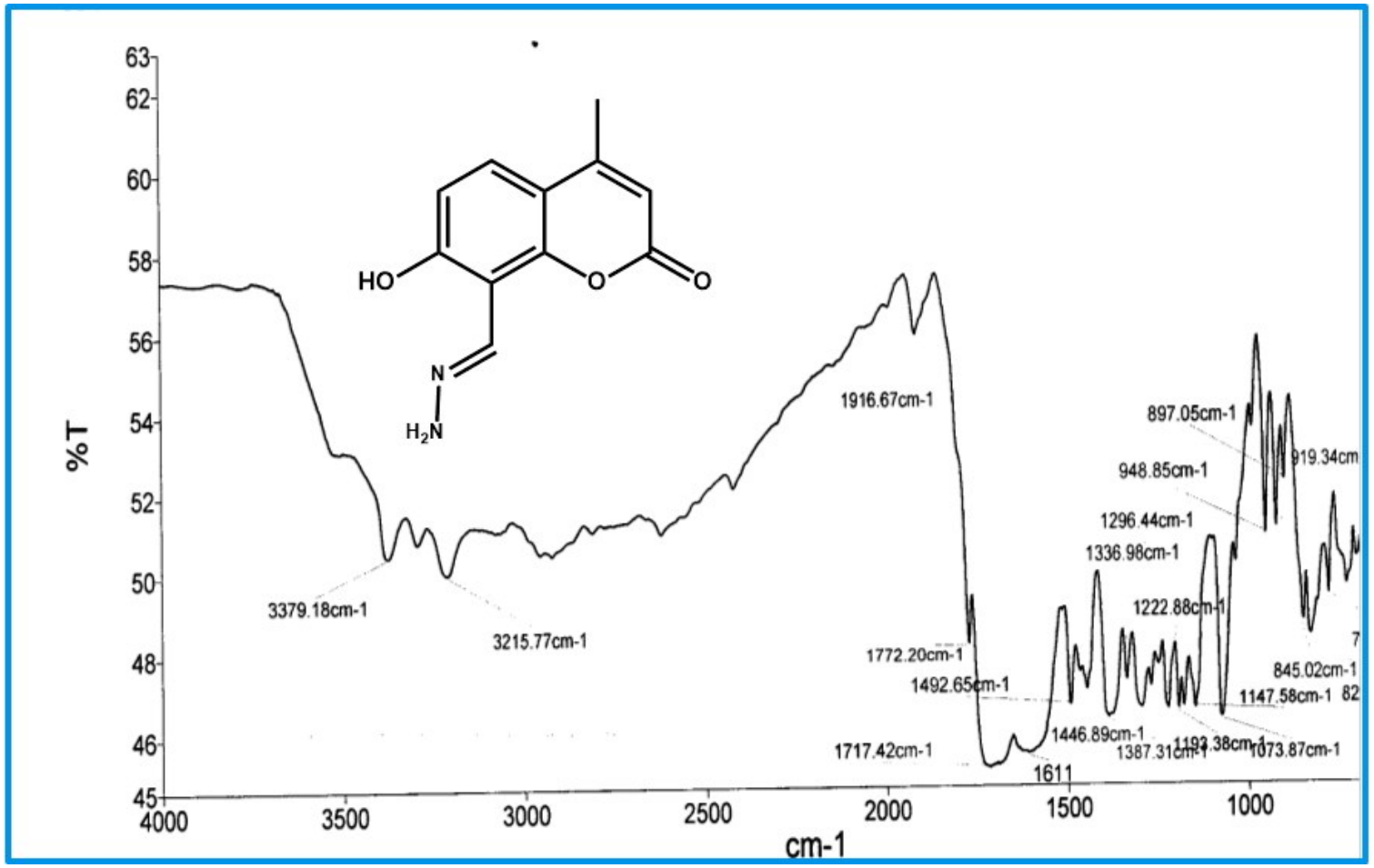

Figure S5: ^{1}H NMR spectrum of **ACM-Hz** (in DMSO-d_6)

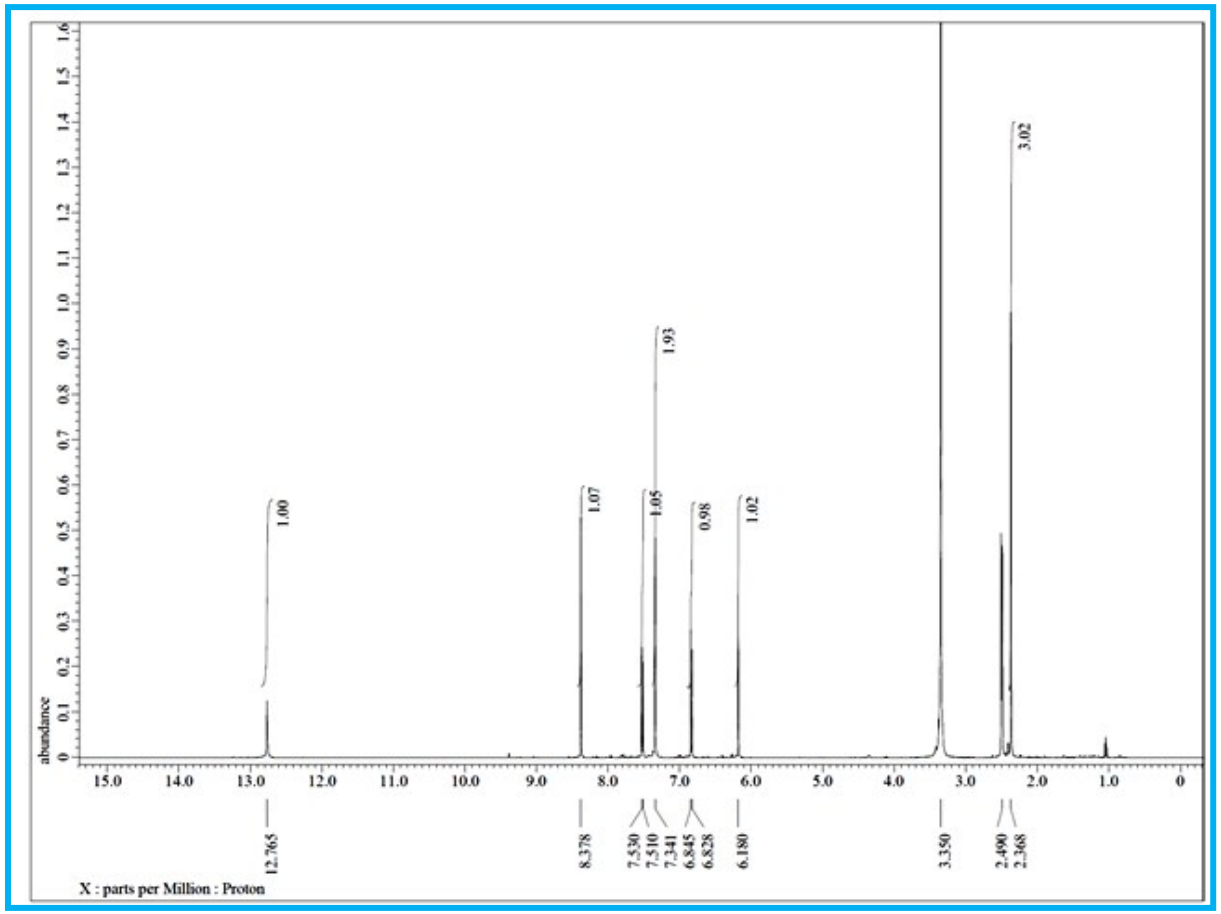

Figure S6: IR spectrum of **CMD**

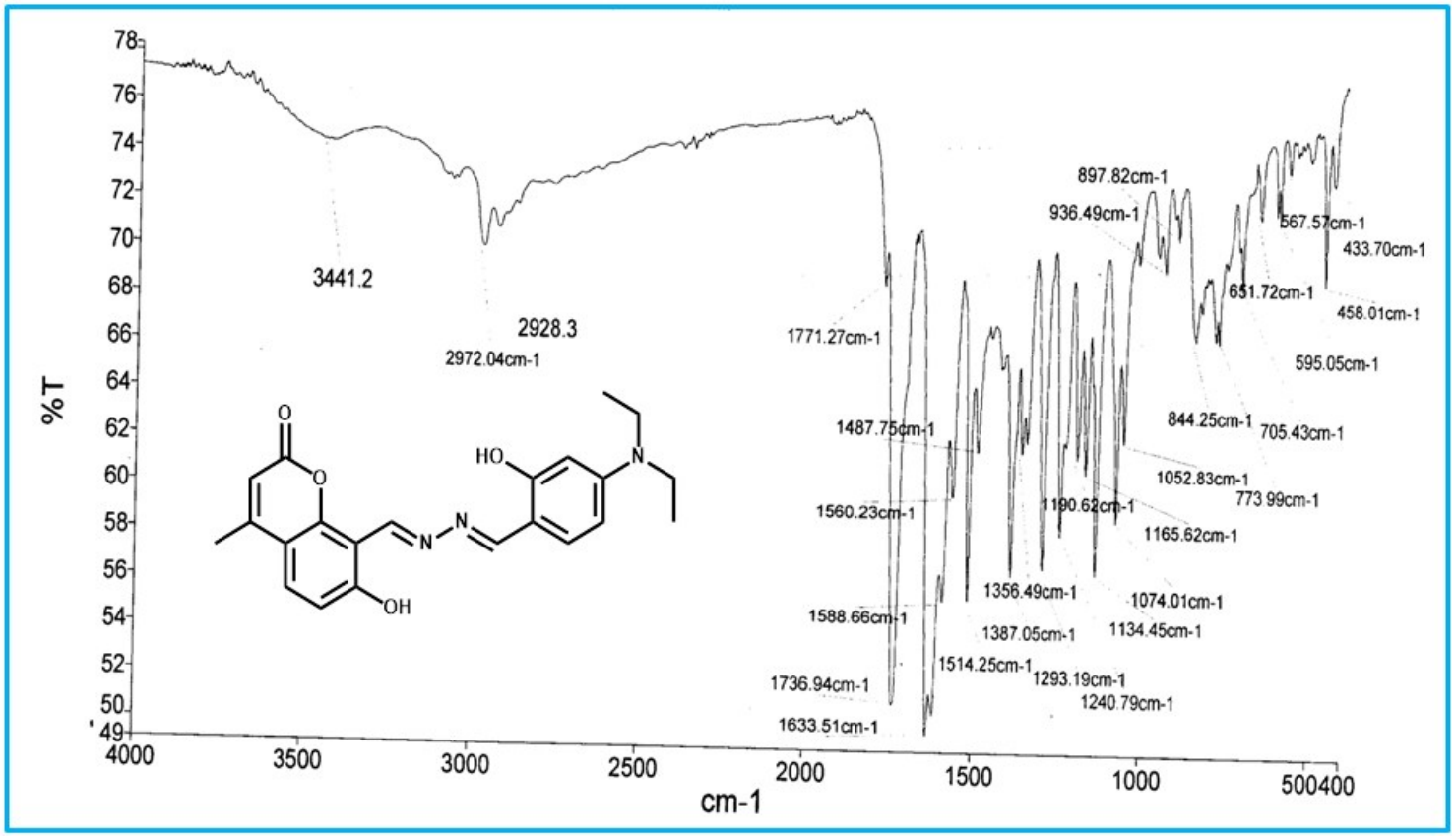

Figure S7: ^{1}H NMR spectrum of **CMD** (in $CDCl_3$)

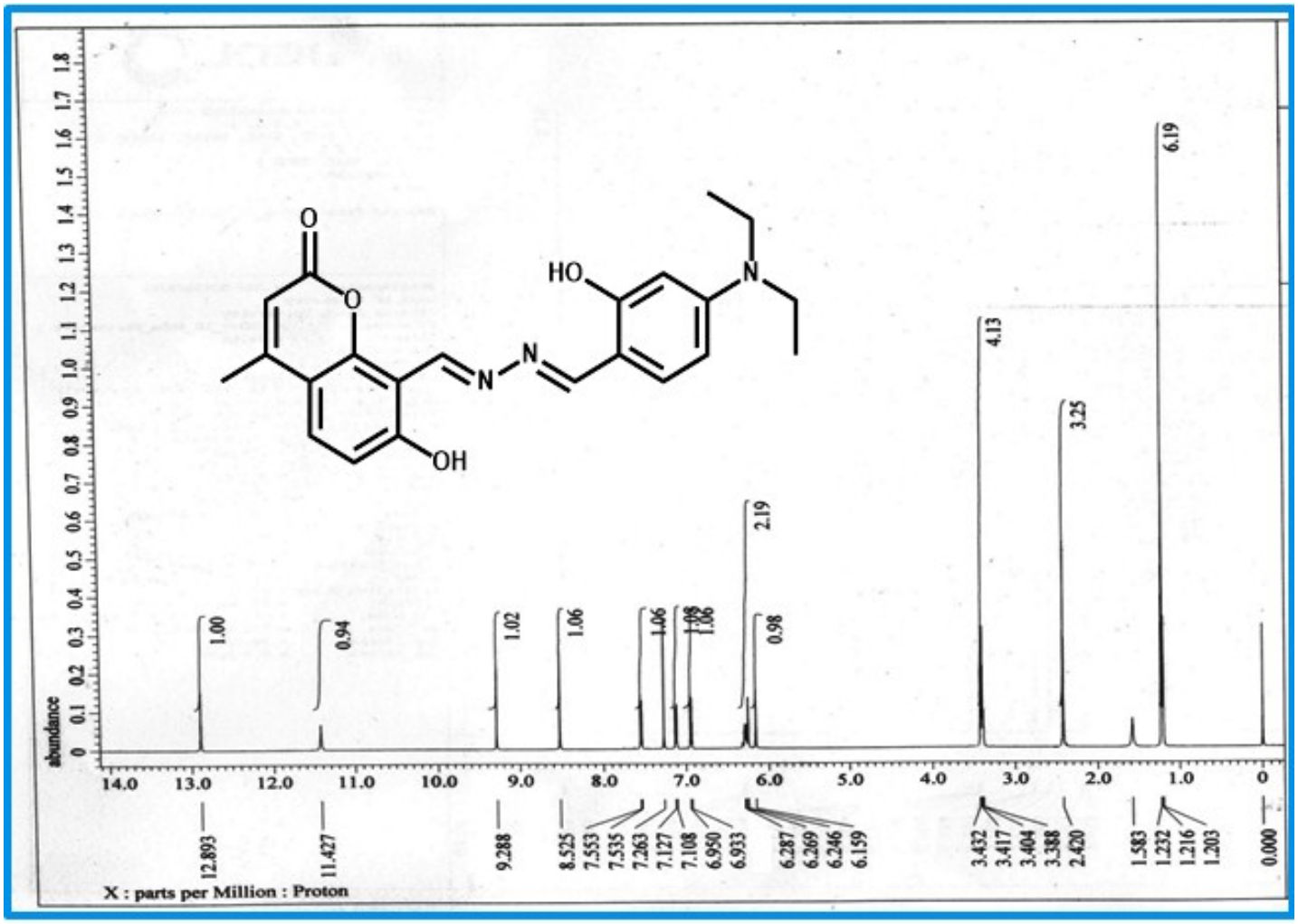

Figure S8: ^{13}C NMR spectrum of **CMD** (in $CDCl_3$)

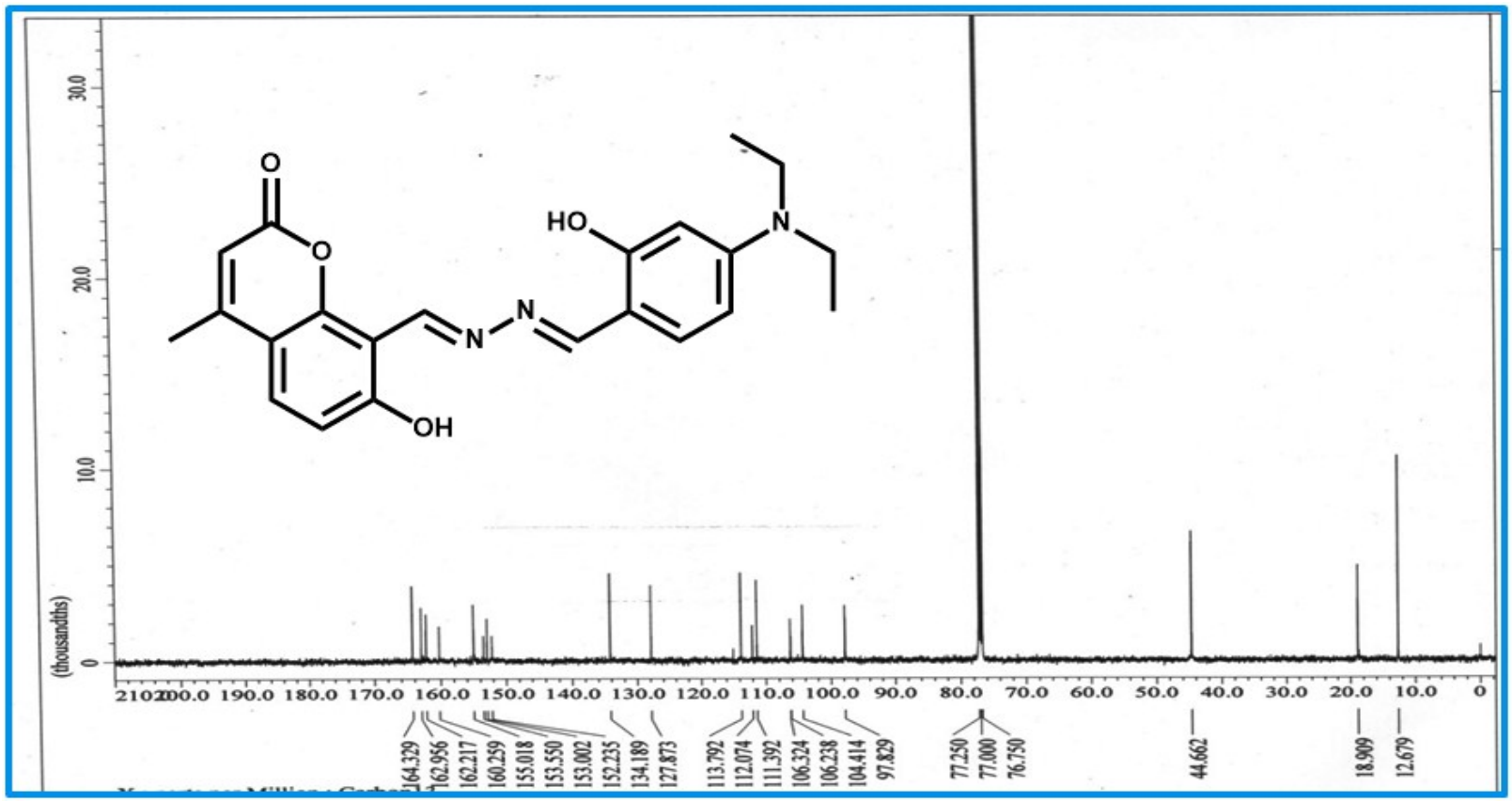

Figure S9: ESI-Mass Spectrum of **CMD**

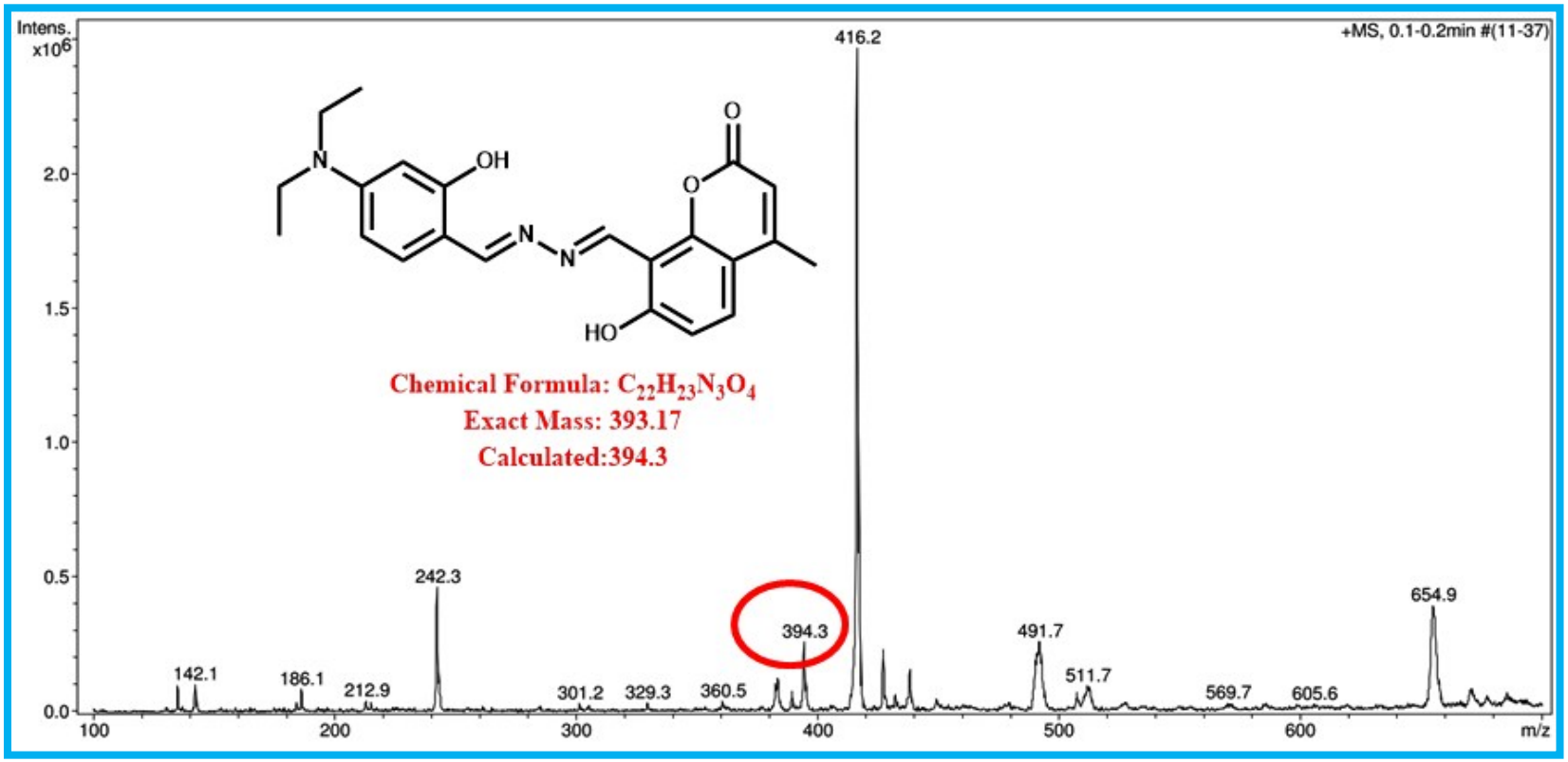

Figure S10: IR spectrum of **CM-Zn-CM'+NSA** crystal

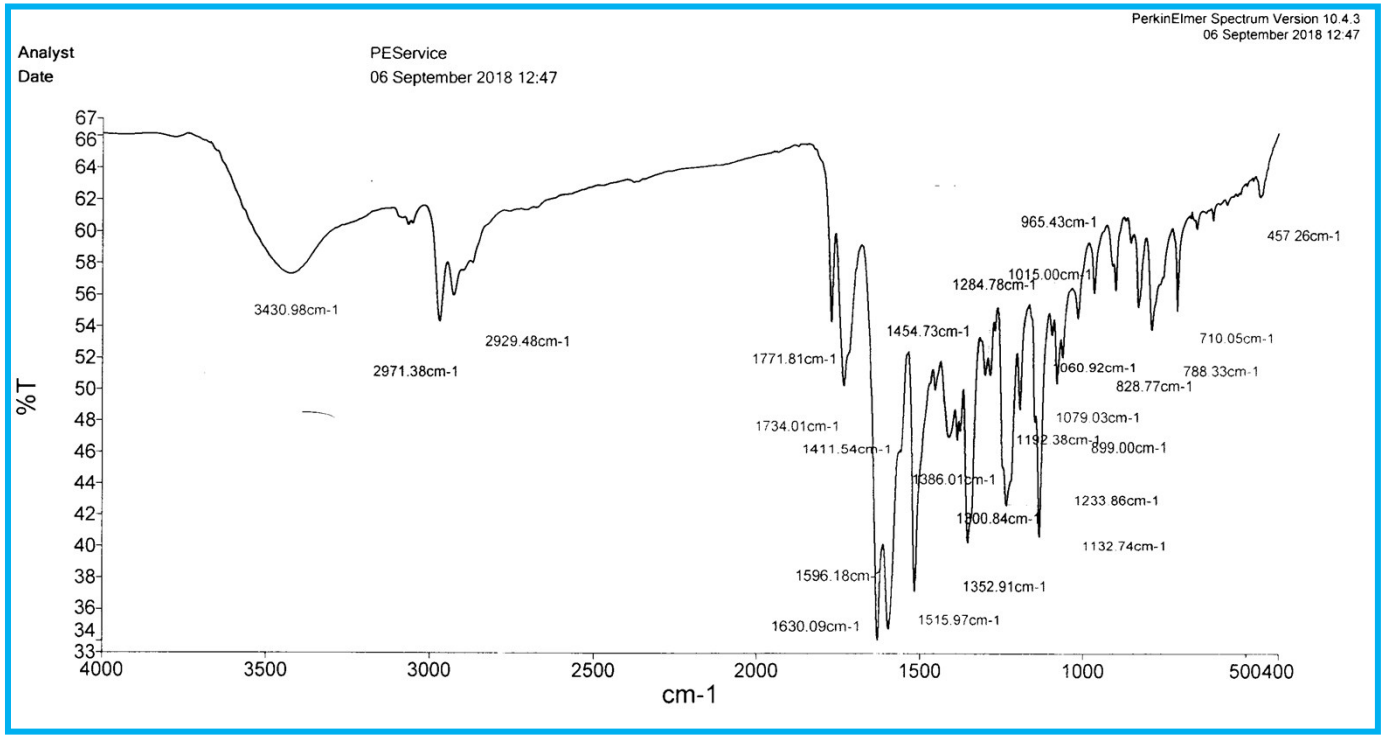

Figure S11: ^{1}H NMR spectrum of crystals of **CM-Zn-CM'+NSA** (in DMSO-d_6)

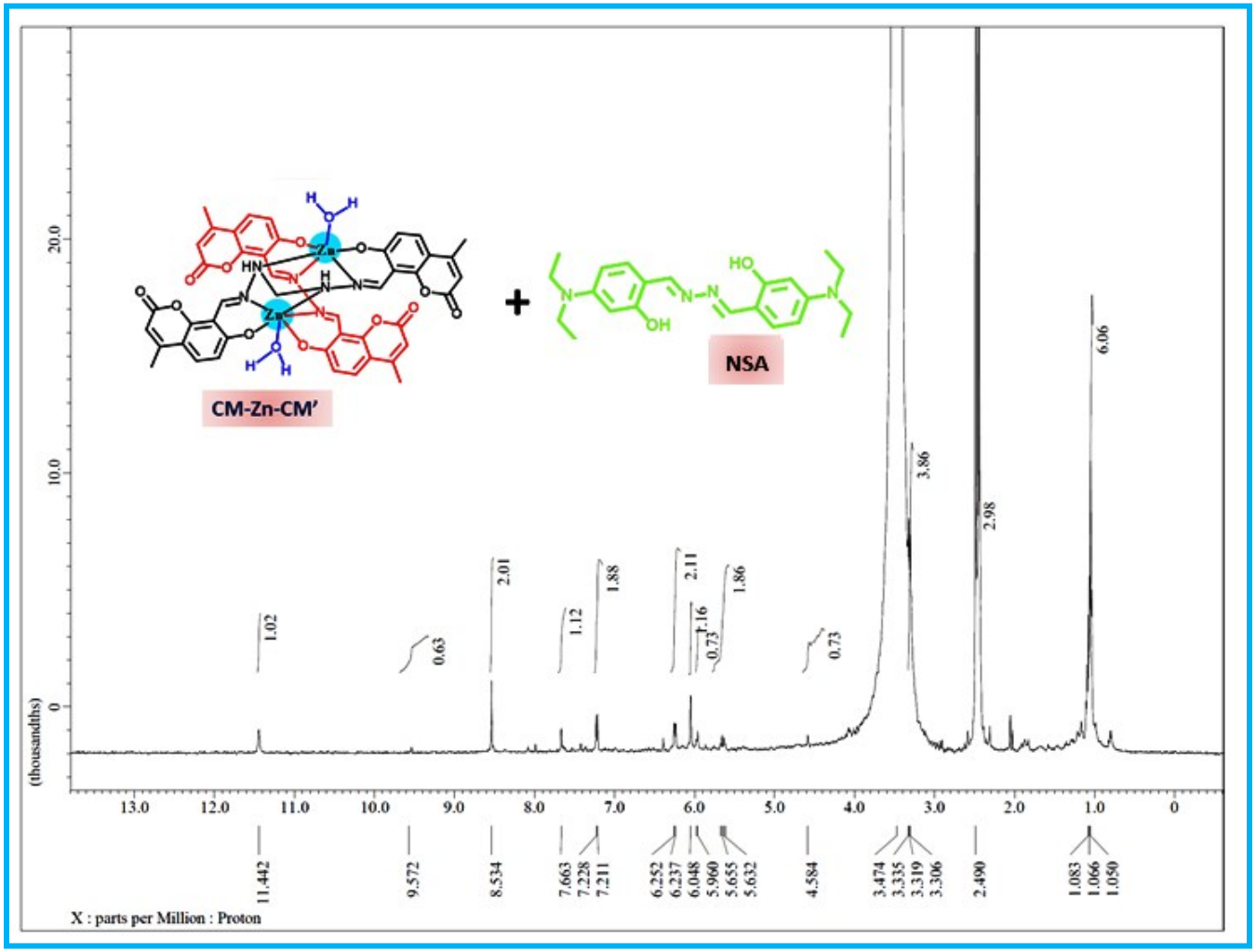

Figure S12: Mass Spectrum of crystals of **CM-Zn-CM'+NSA.**

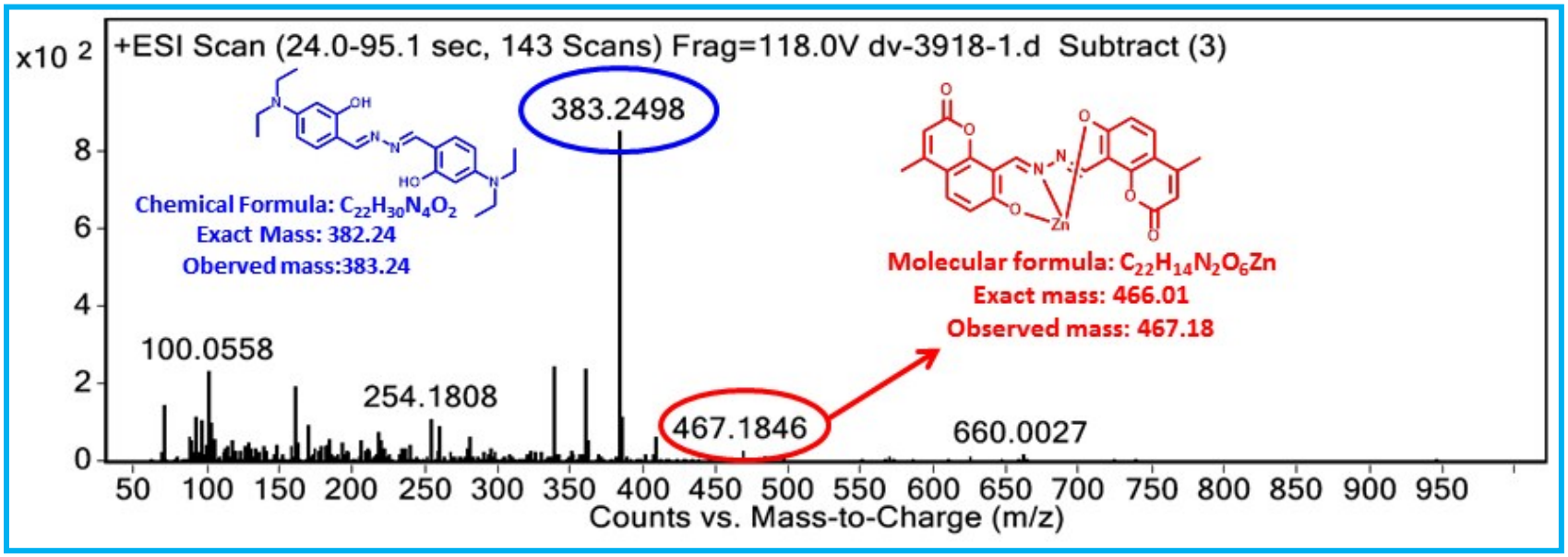

Figure S13: IR spectrum of **NSA**

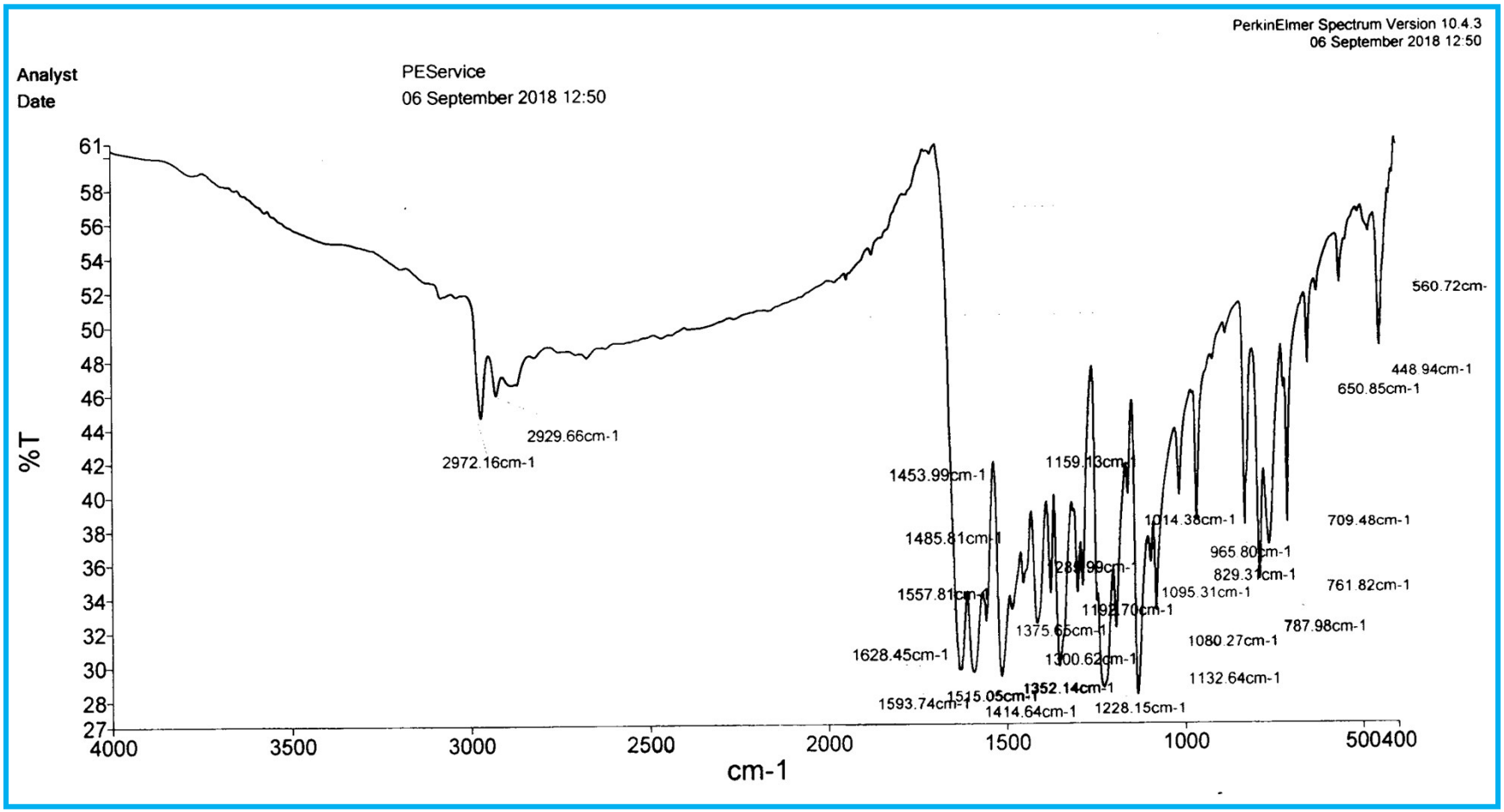

Figure S14: ^{1}H NMR spectrum of **NSA** (in DMSO-d_6)

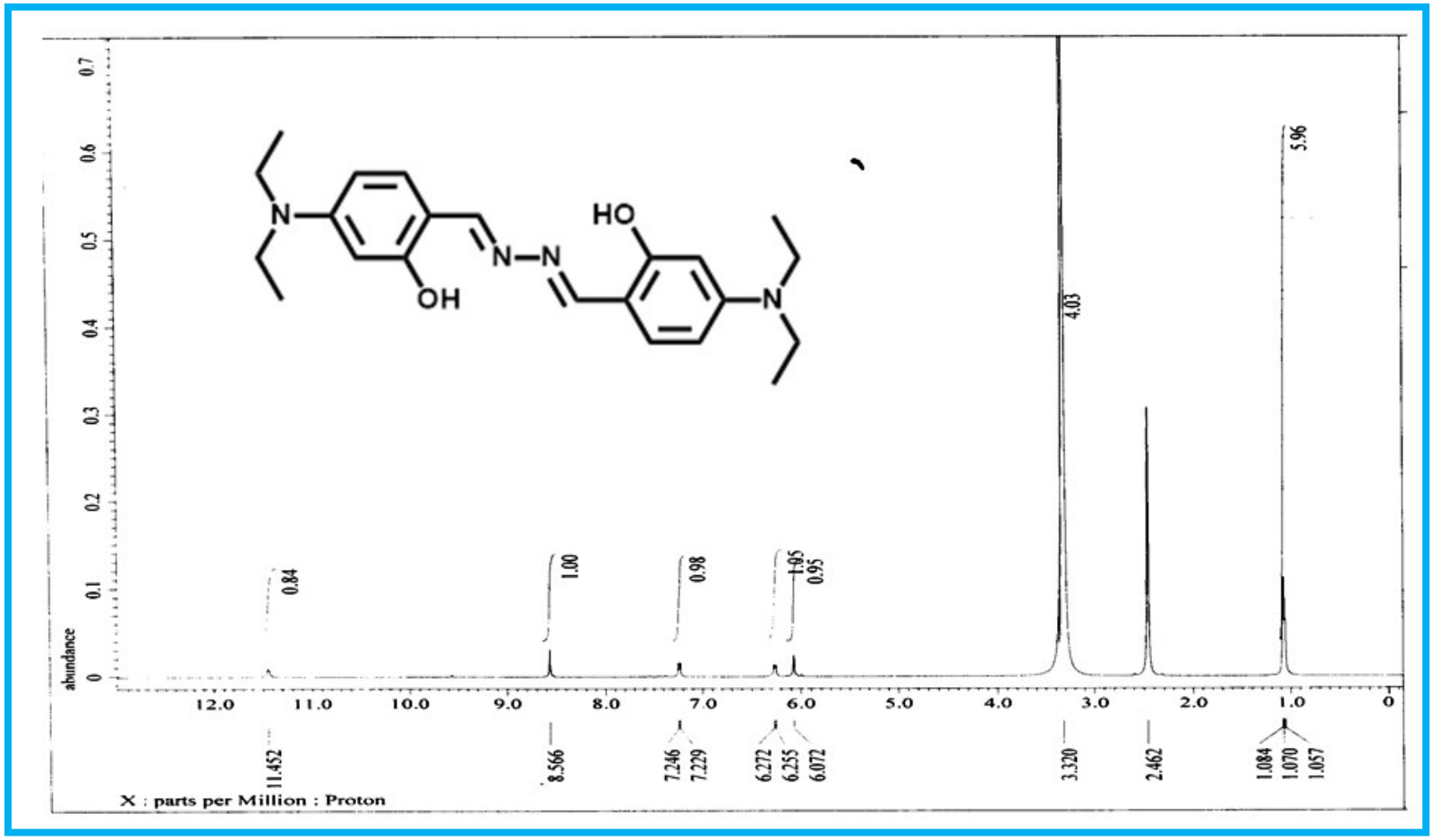

Figure S15: ^{13}C NMR spectrum of **NSA** (in DMSO-d_6)

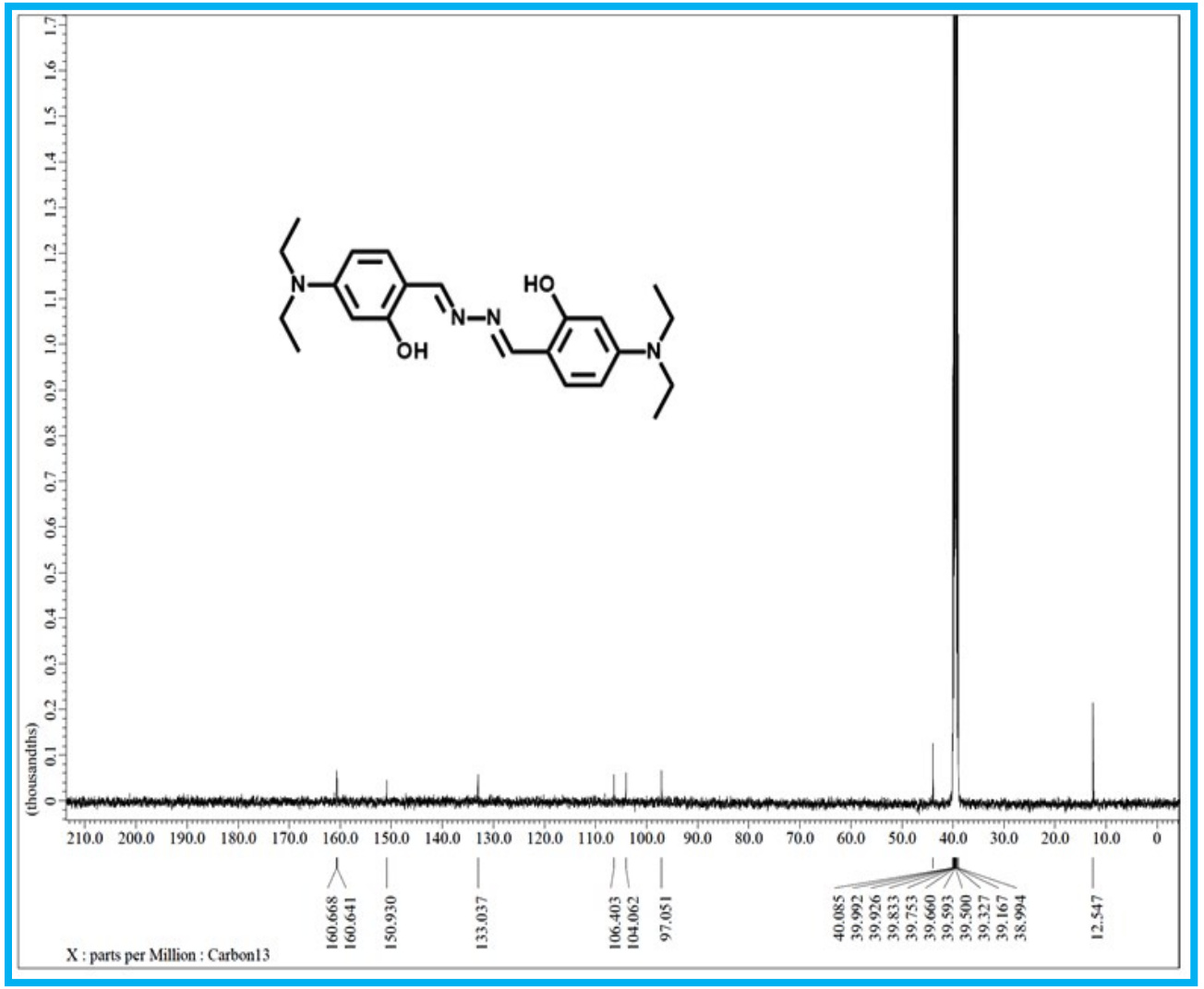

Figure S16: Mass Spectrum of **NSA**

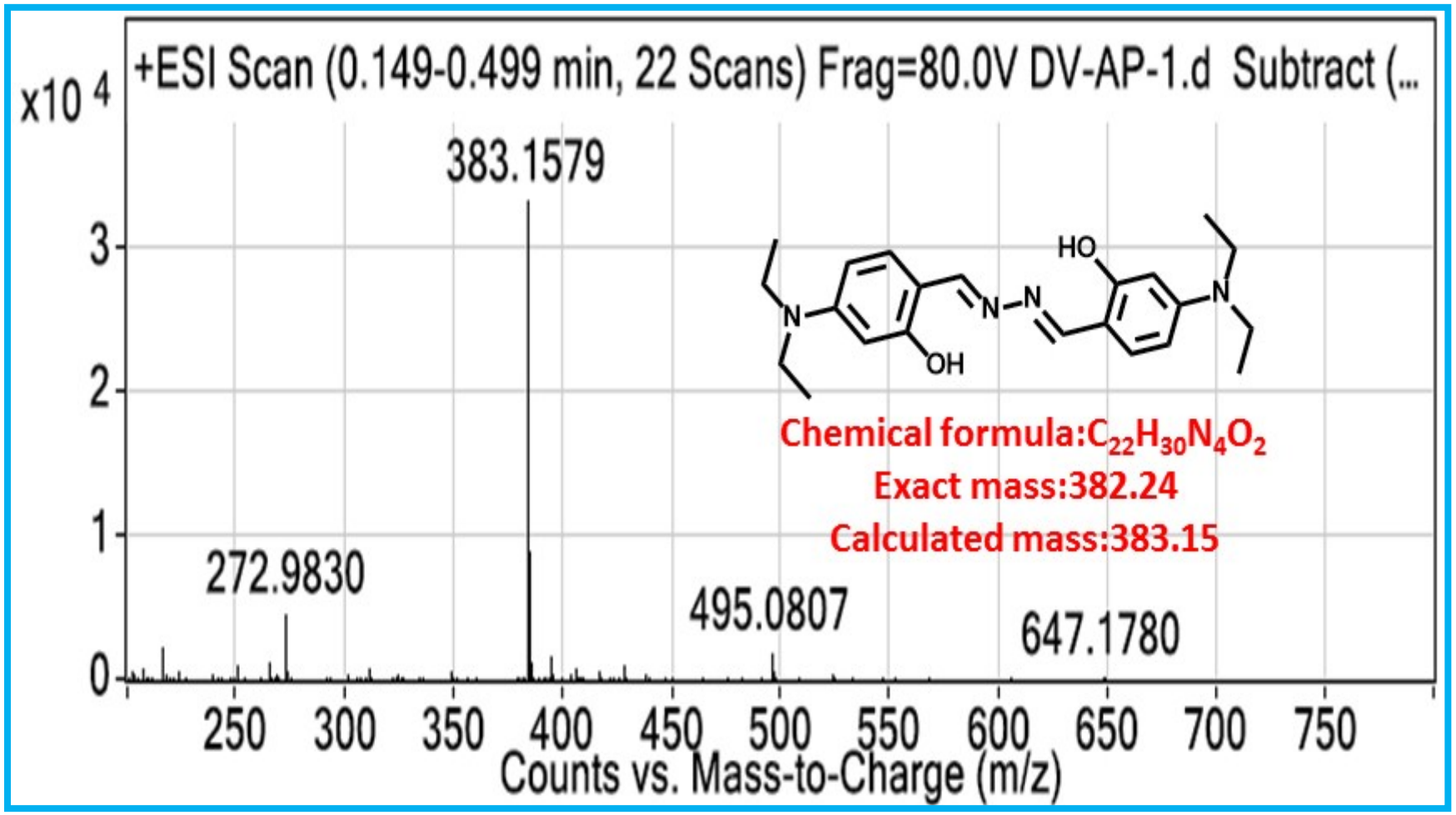

Figure S17: IR spectrum of **CM**

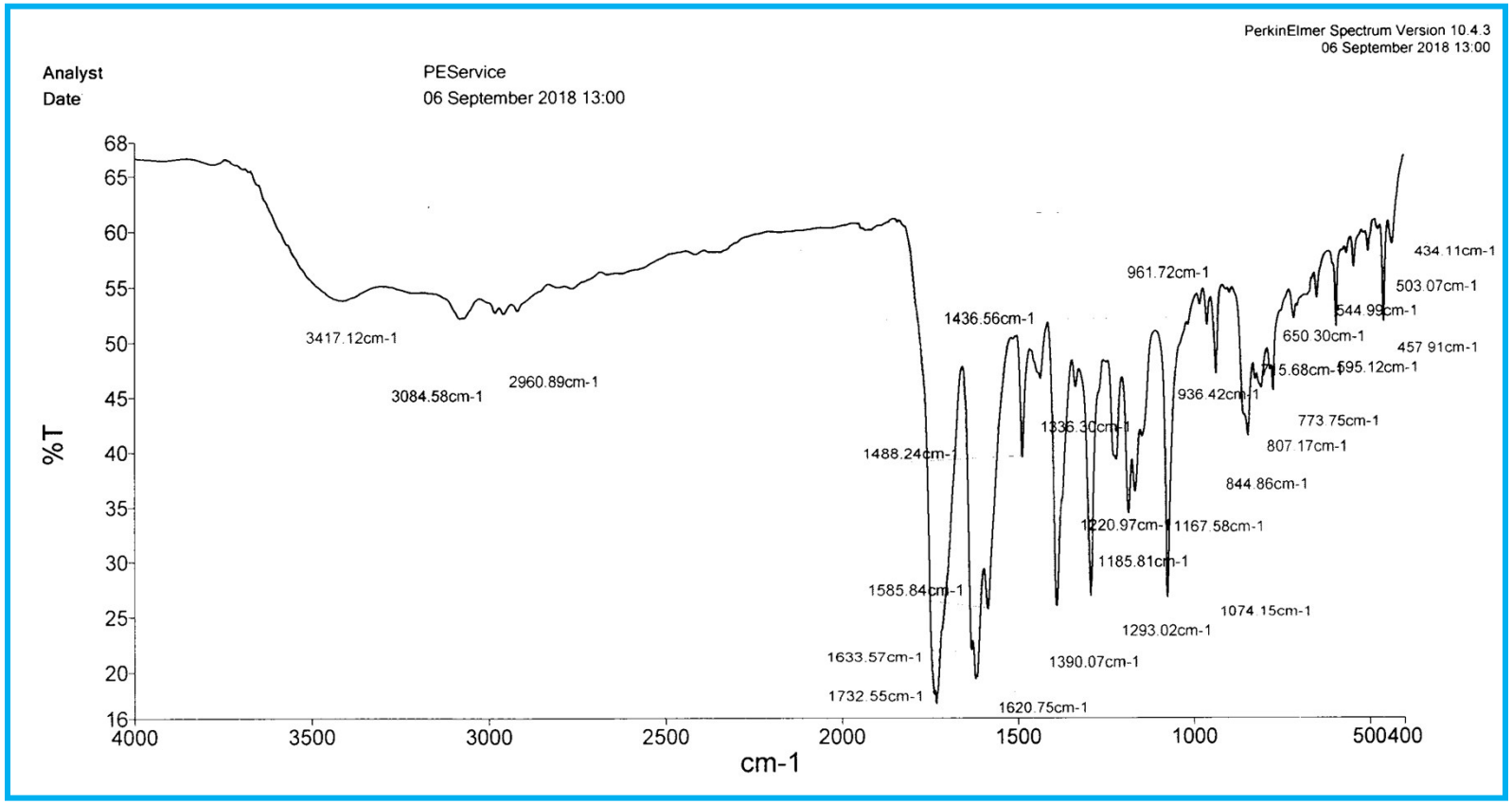

Figure S18: ^{1}H NMR spectrum of **CM** (in DMSO-d_6)

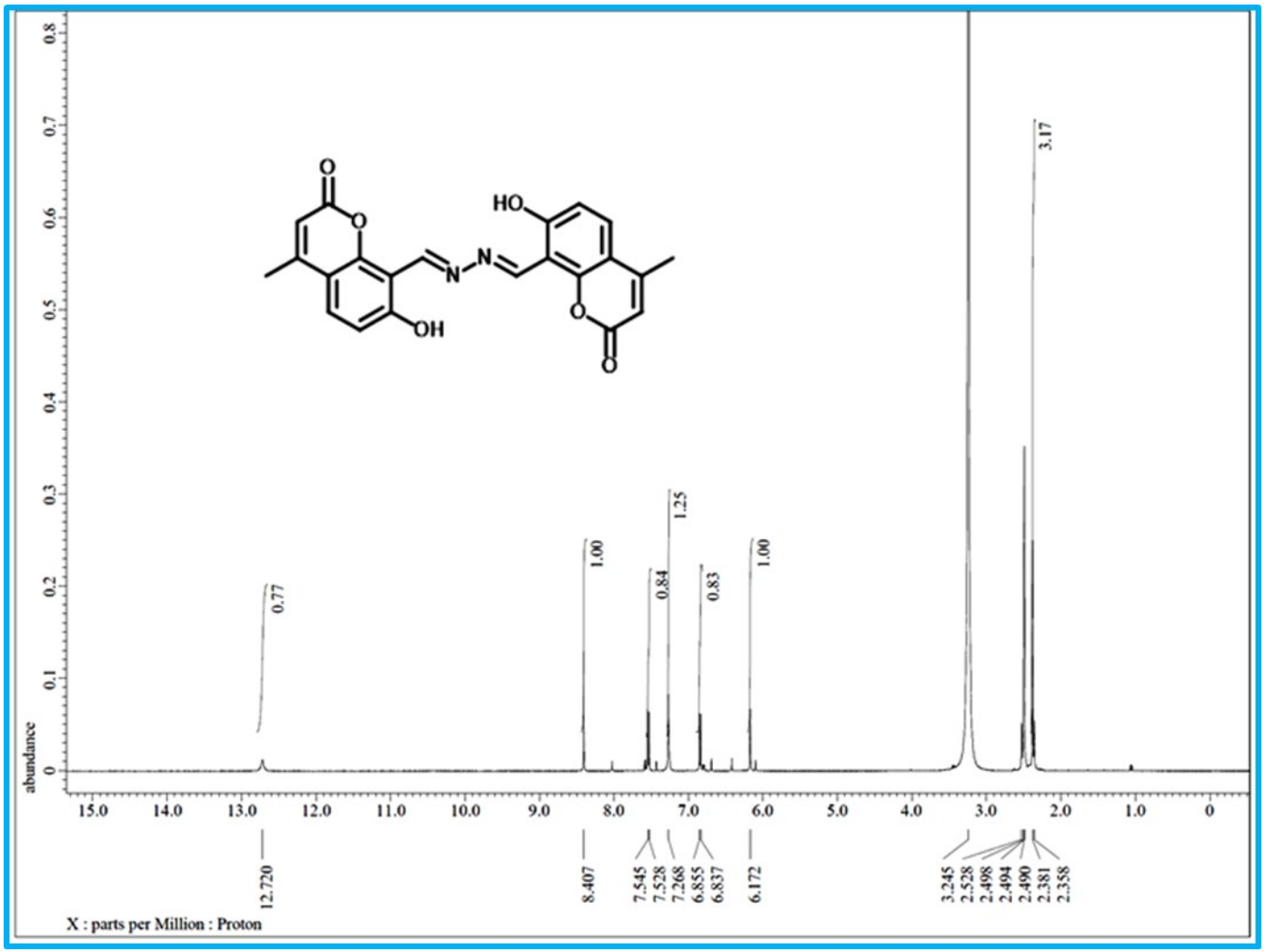

Figure S19: ^{13}C NMR spectrum of **CM** (in DMSO-d_6)

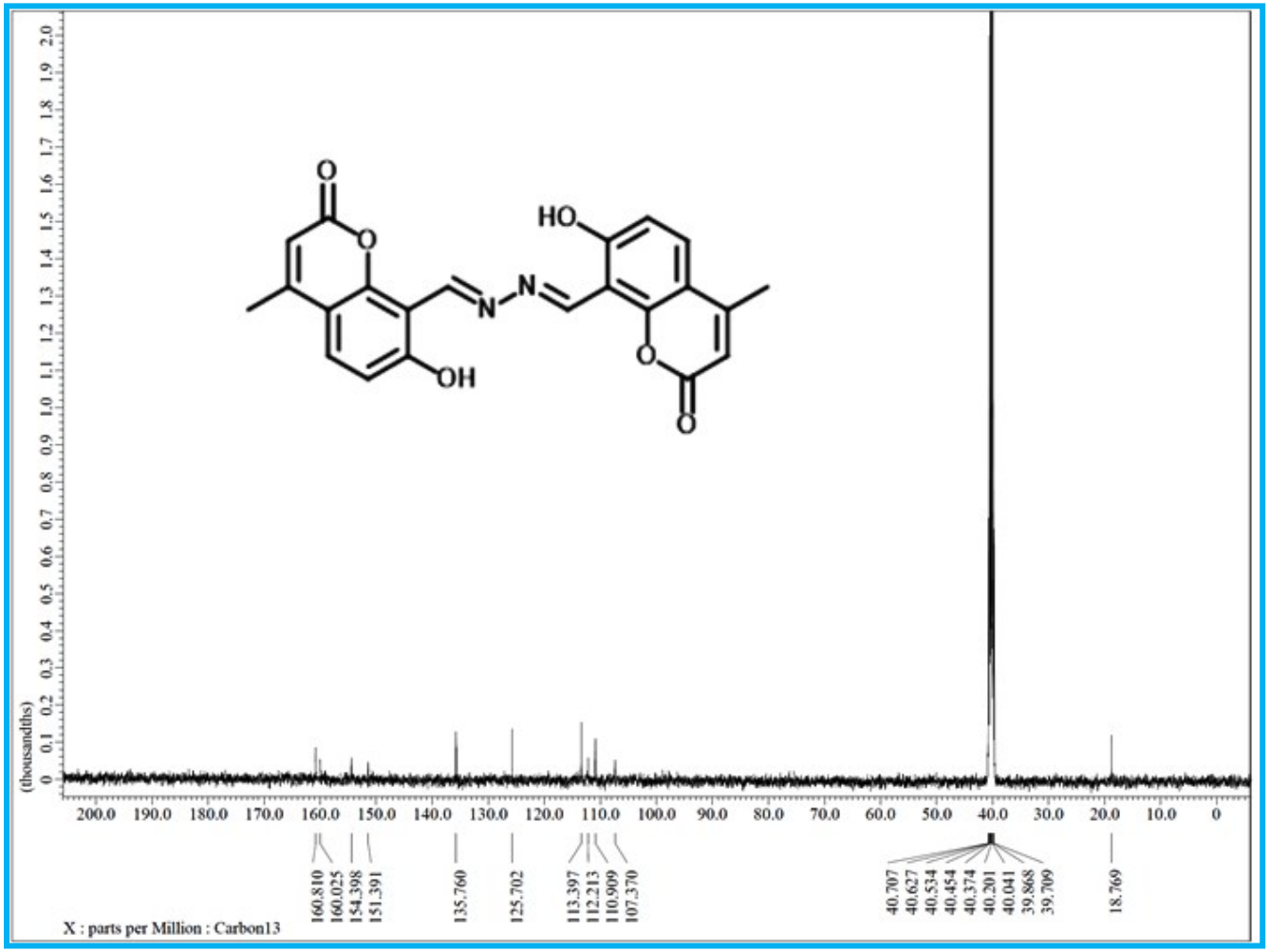

Figure 20: ESI-Mass Spectrum of **CM**

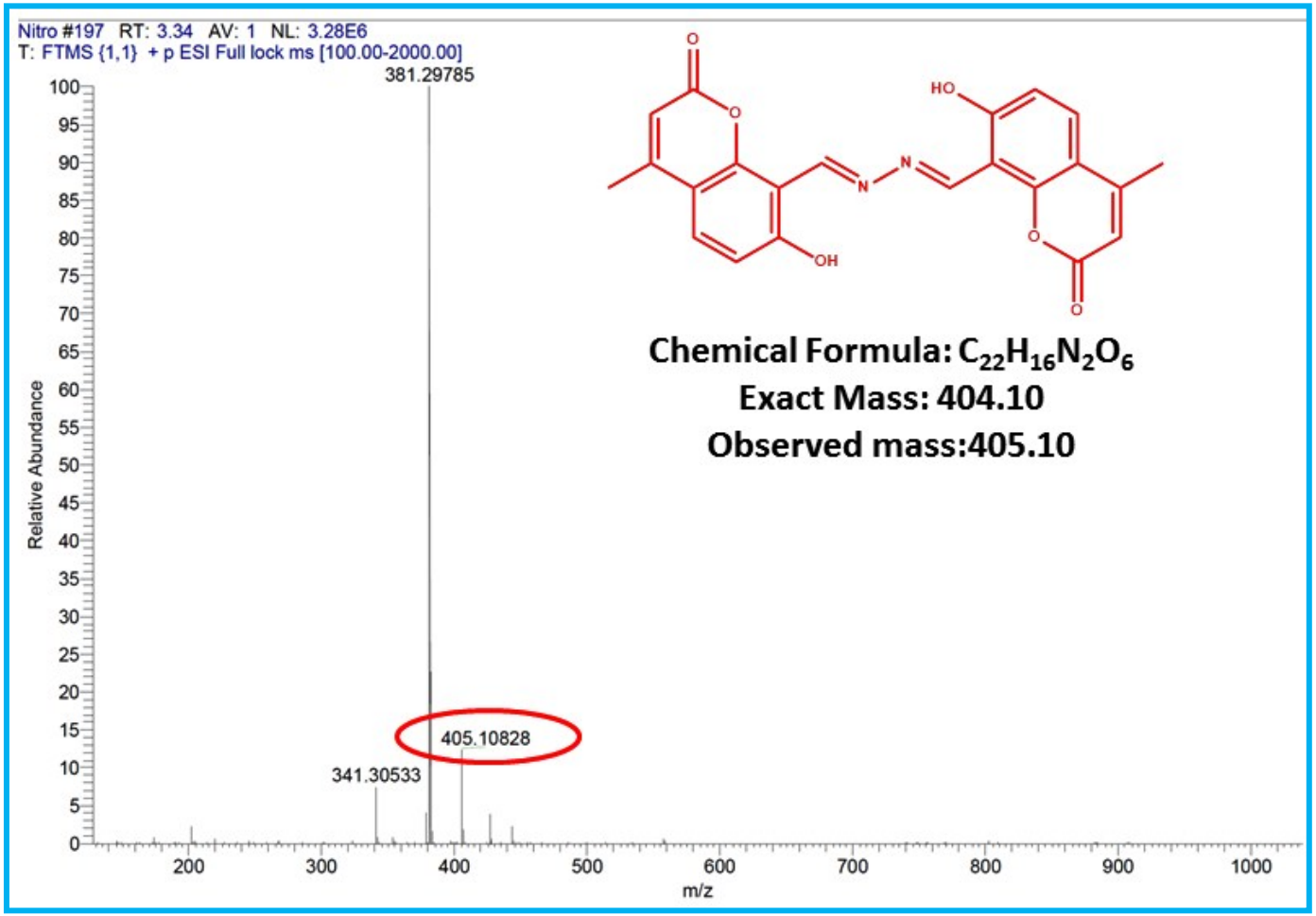

Figure S21: IR spectrum of **CM-Zn-CM**

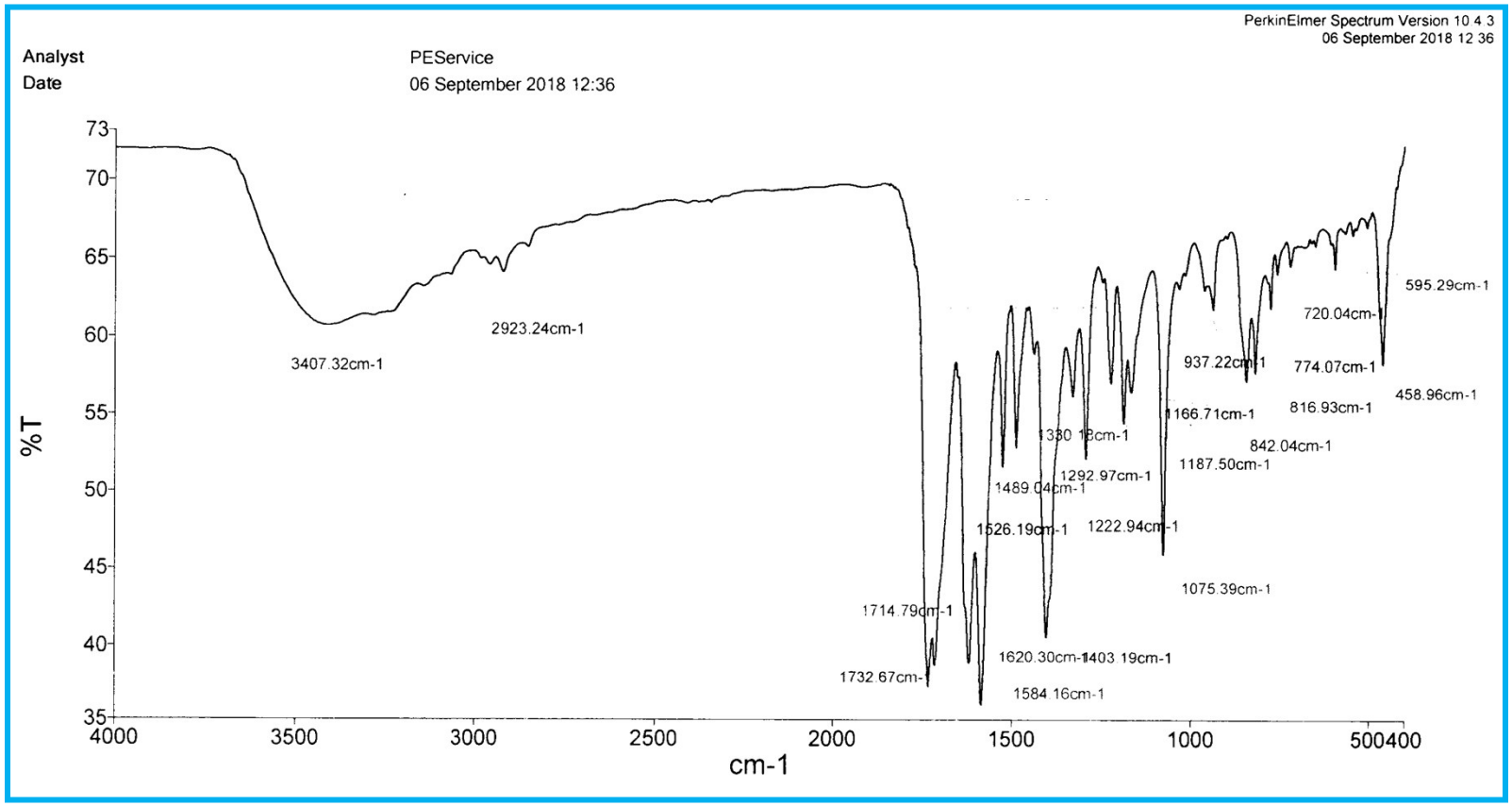

Figure S22: ^{1}H NMR spectrum of **CM-Zn-CM** (in DMSO-d_6)

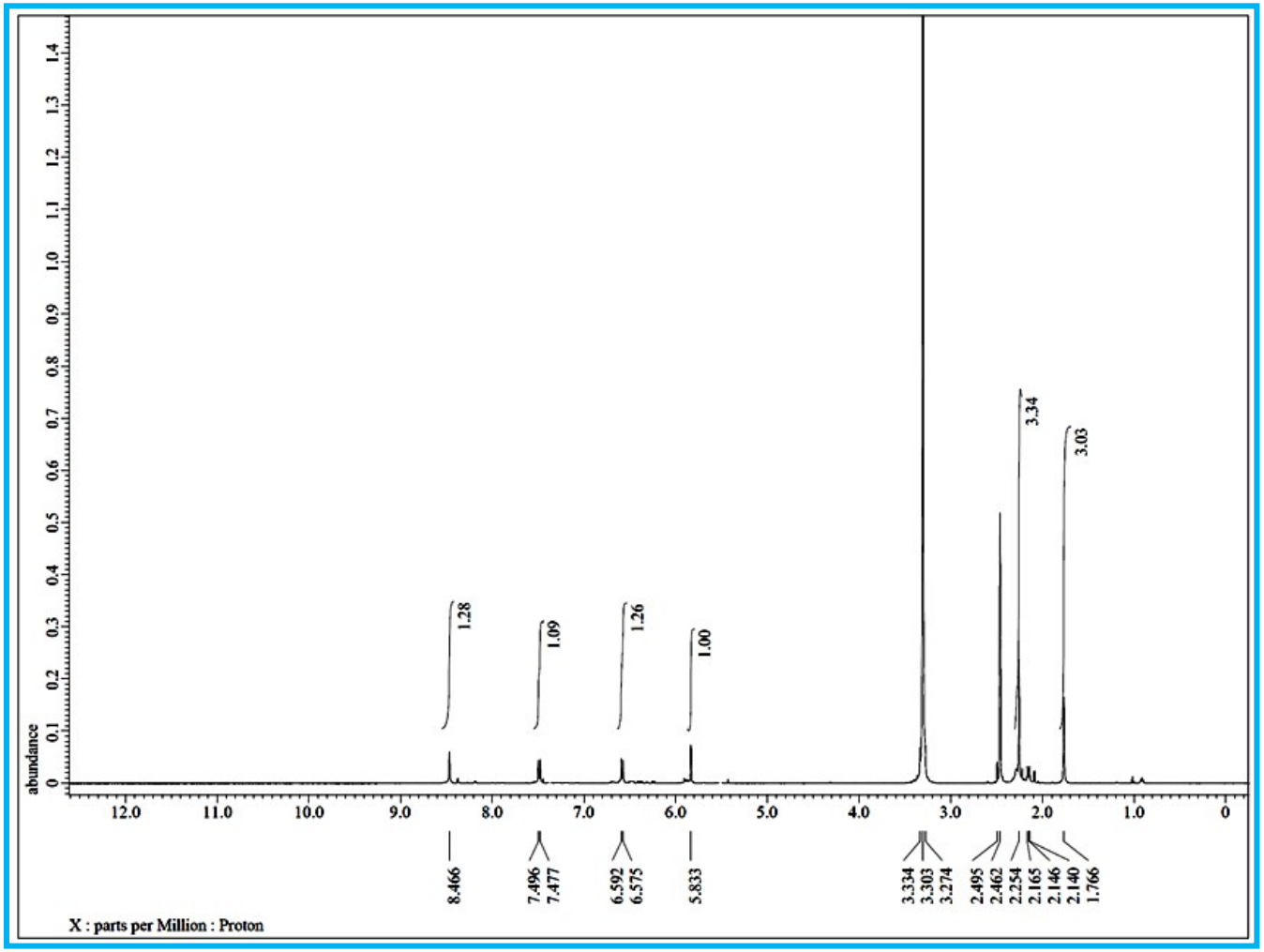

Figure S23: ^{13}C NMR spectrum of **CM-Zn-CM** (in DMSO-d_6)

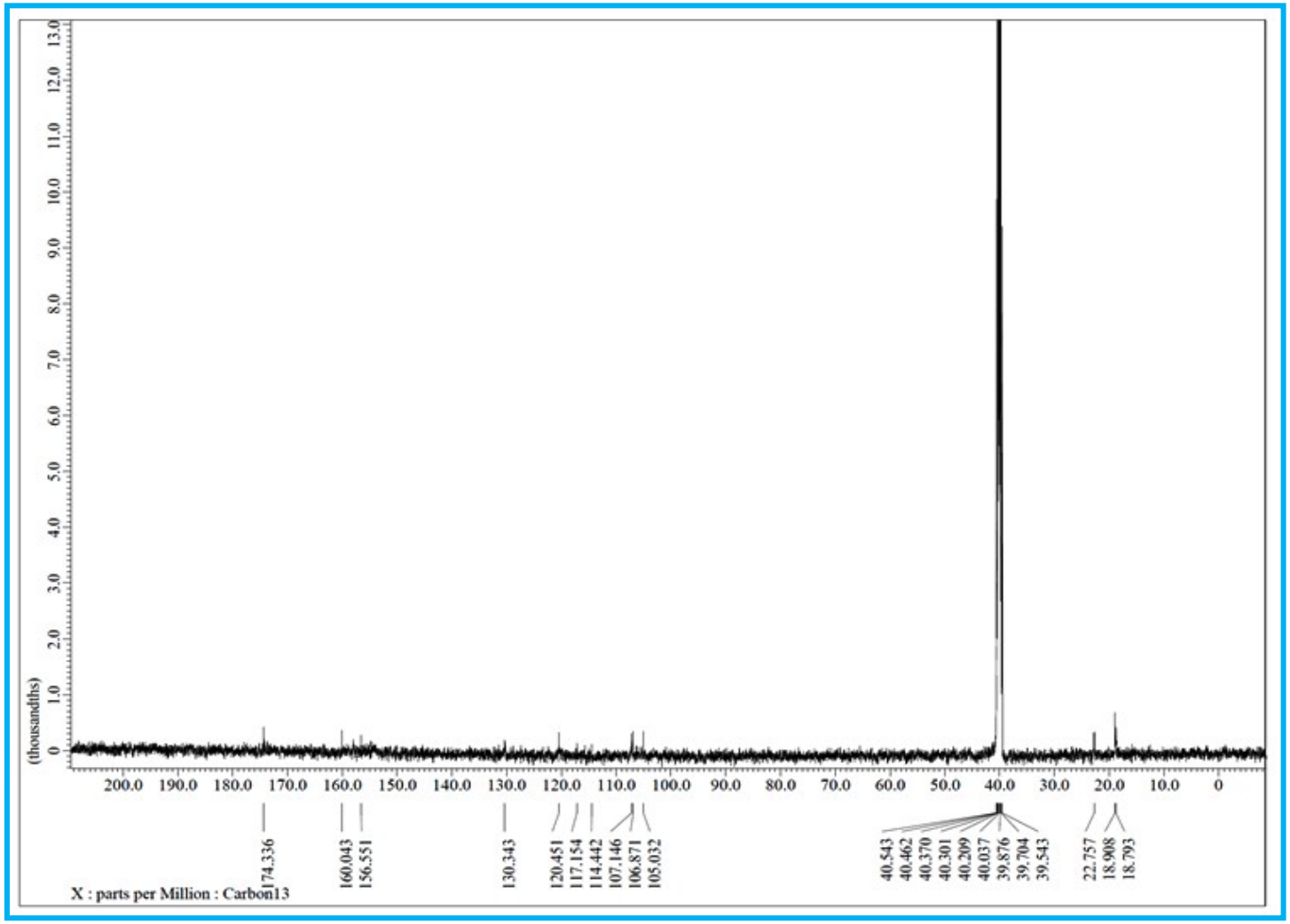

Figure S24: Solid state fluorescence spectra of **CMD (**λex = 420 nm**)** and **NSA** (λex = 425 nm).

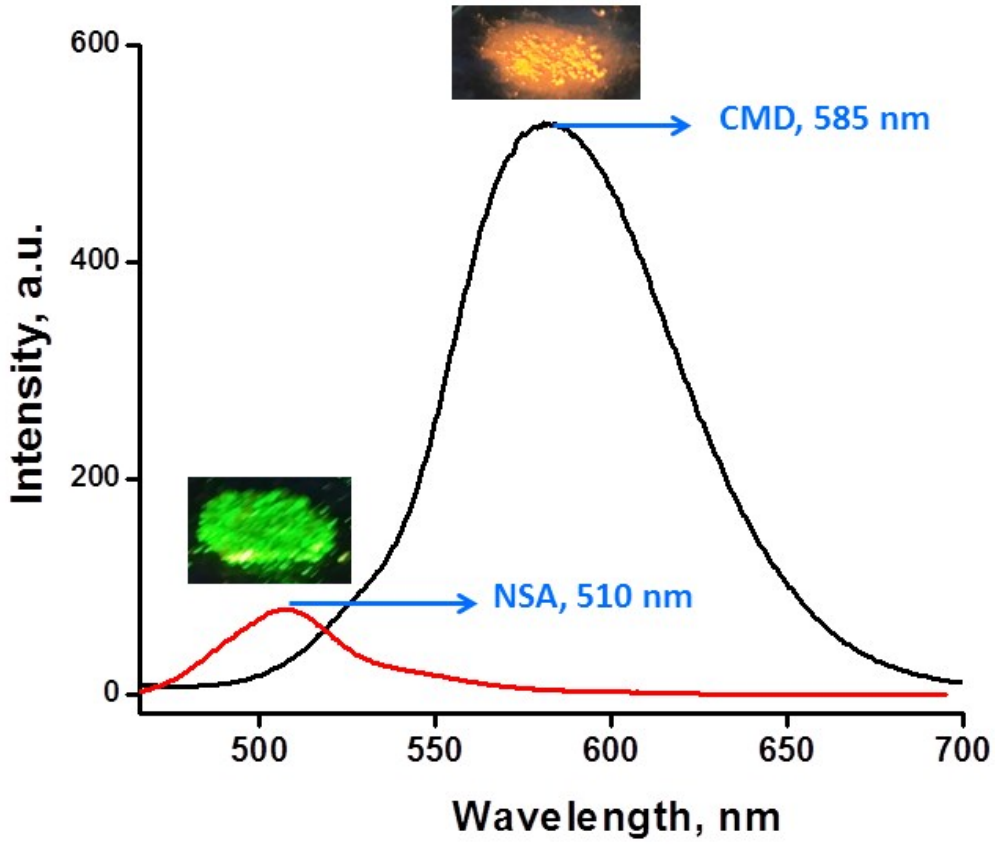

Figure S25: (a) Supramecular architecture showing 2D layer based inter-chain H-bondings (b) Torsion of phenyl ring and coumarin ring at an angle of ~4°. (c) Crystal structure of **CMD** showing π–π stacking interaction into head-to-tail arrangement. (d) Hydrogen bonds between π-stacked columns.

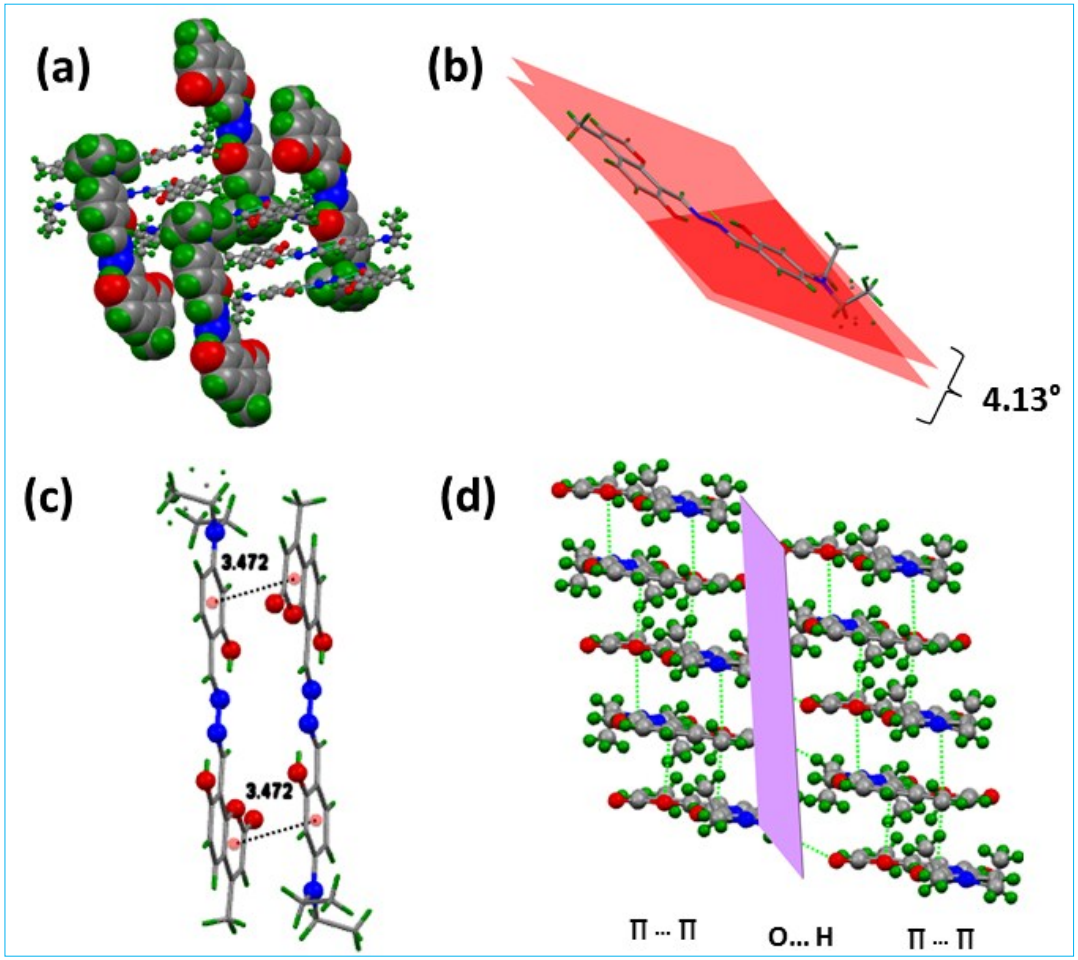

Scheme S1: Showing crystallizing mechanism of complex of **CMD** with zinc acetate in DMSO+ethanol mixture after layering with Dichloromethane

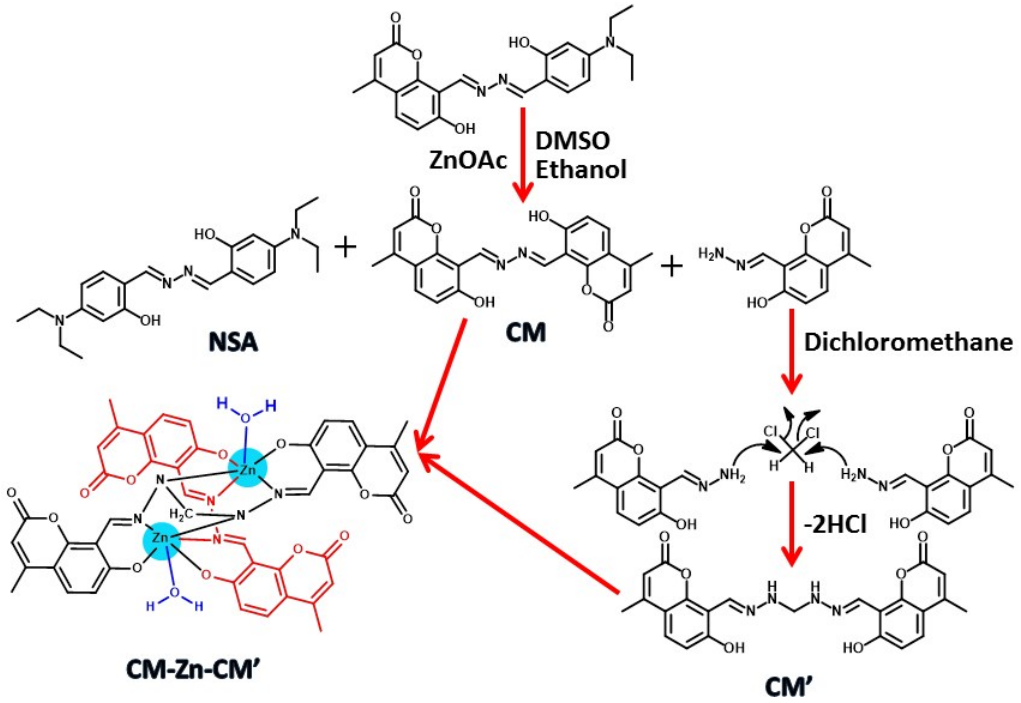

Figure S26: showing ortep view of a single crystals of **NSA** with displacement ellipsoids at 50% probability.

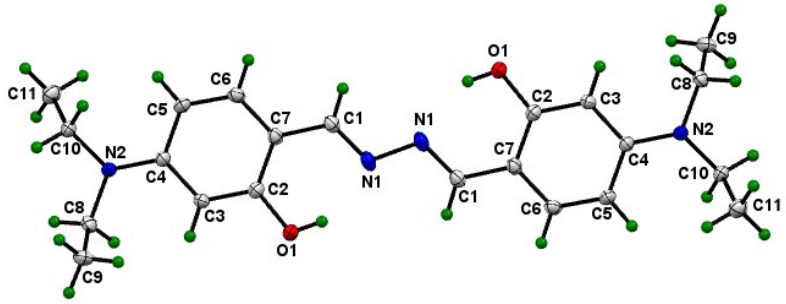

Figure S27 (a): UV-vis spectra of **CMD** (10 μM) in Ethanol upon addition of Zn^{2+} (10 equiv.)

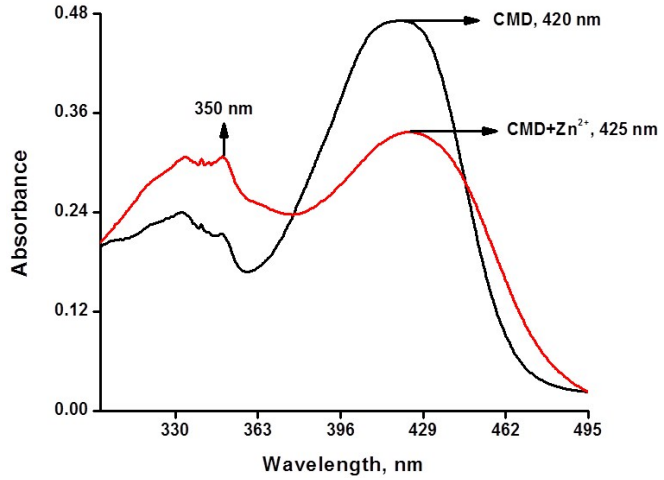

Figure S27 (b): UV-vis titration spectra of **CMD** (10 μM) in Ethanol upon concomitant addition of Zn^{2+} (0-17.5 equiv.)

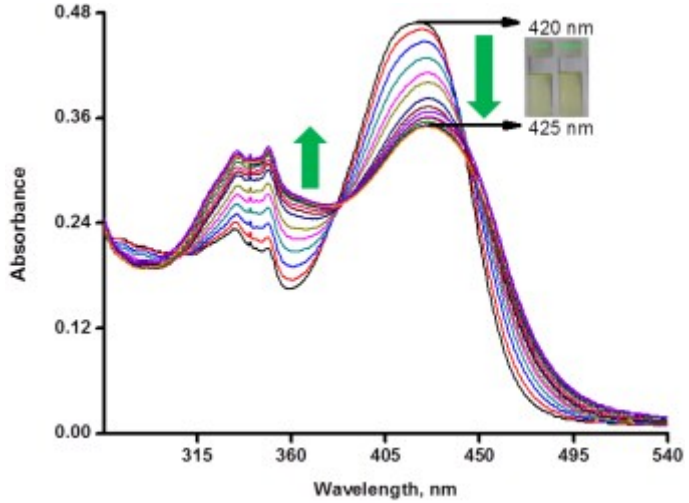

Figure S28 (a): Photograph showing naked eye color change of **CMD** (10 μM) under visible (365 nm) light in presence of different metal ions

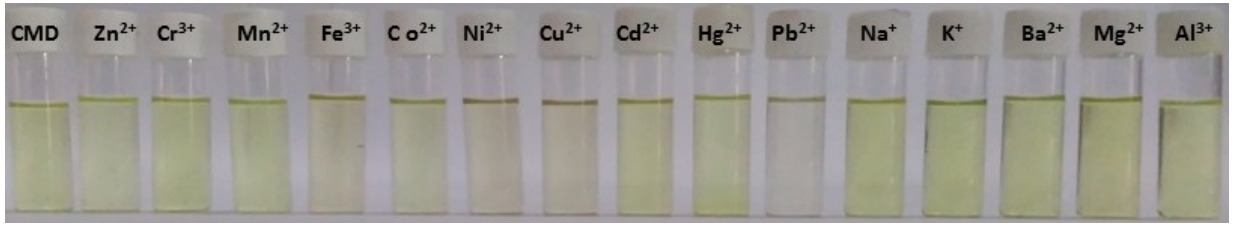

Figure S28(b): UV-visible spectrum of **CMD** (10 μM) with different metal ions (10 equiv.) in Ethanolic medium

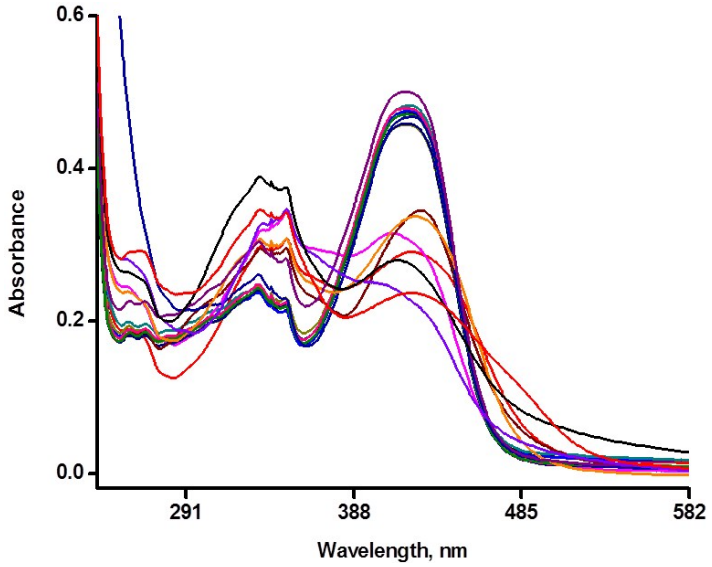

Figure S29: Schematic representation of **CMD** showing quenching of PET phenomenon due to intramolecular hydrogen bonding

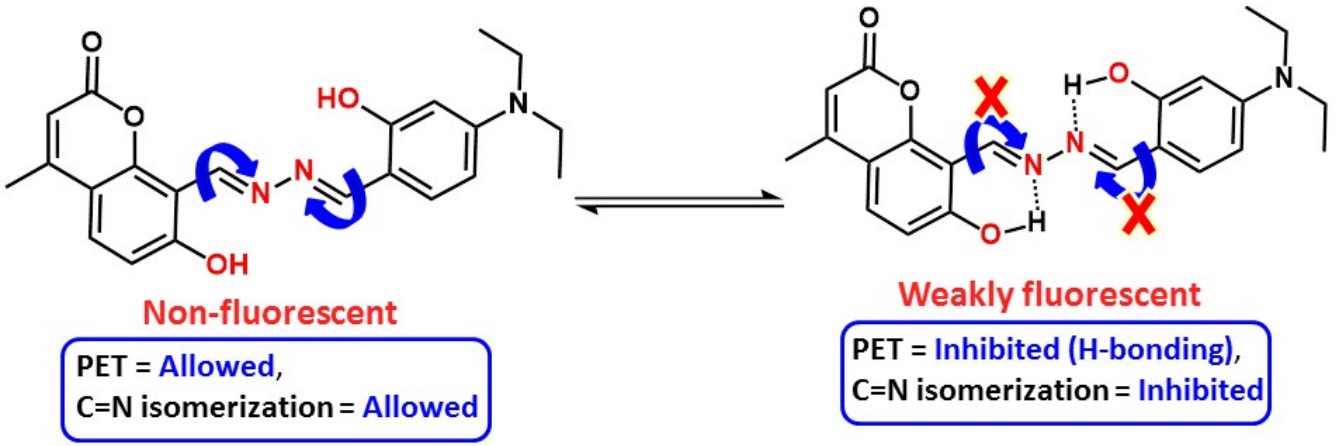

Figure S30: Fluorescence spectra showing effect of counter anions of zinc on the fluorescence behaviour of **CMD**

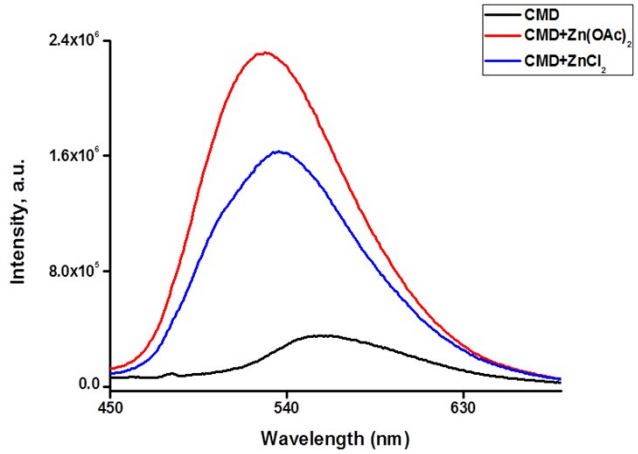

Figure S31: Reaction-time profile of **CMD (**1 μM**)** in presence of ZnOAc (10 equiv.)

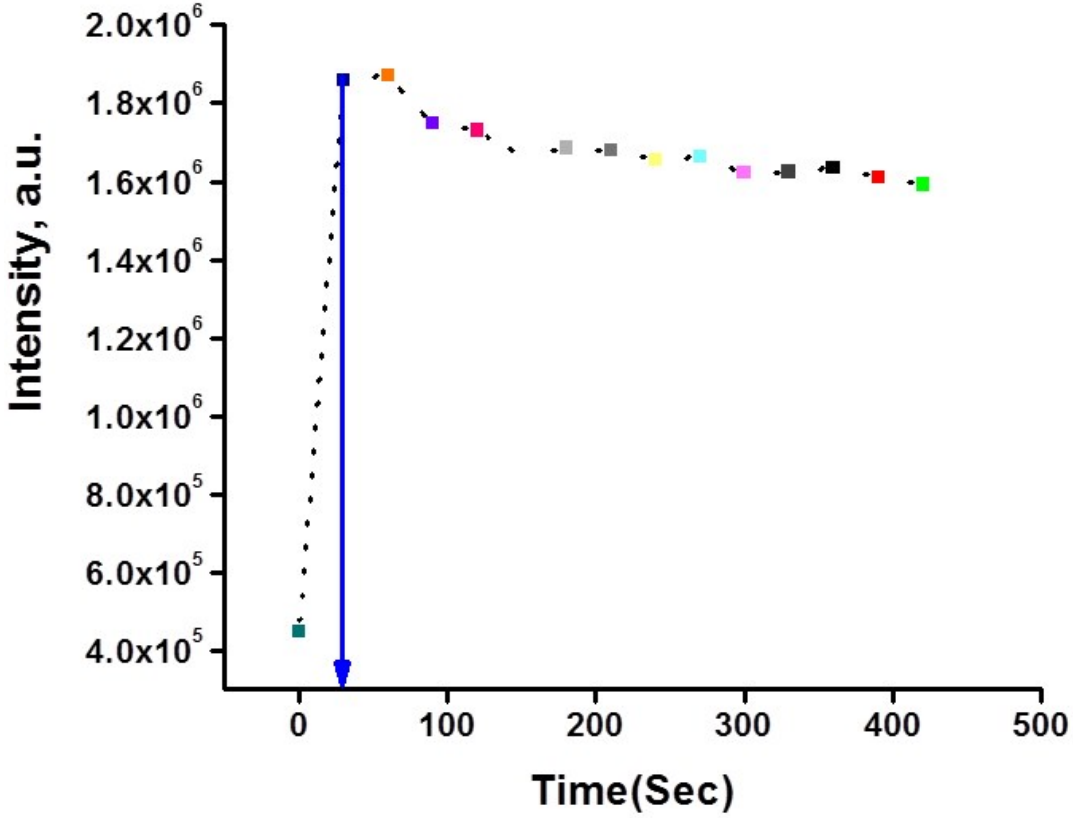

Figure S32: Calibration curve for determination of detection limit of **CMD** for Zn^{2+} by fluorescence titration data.

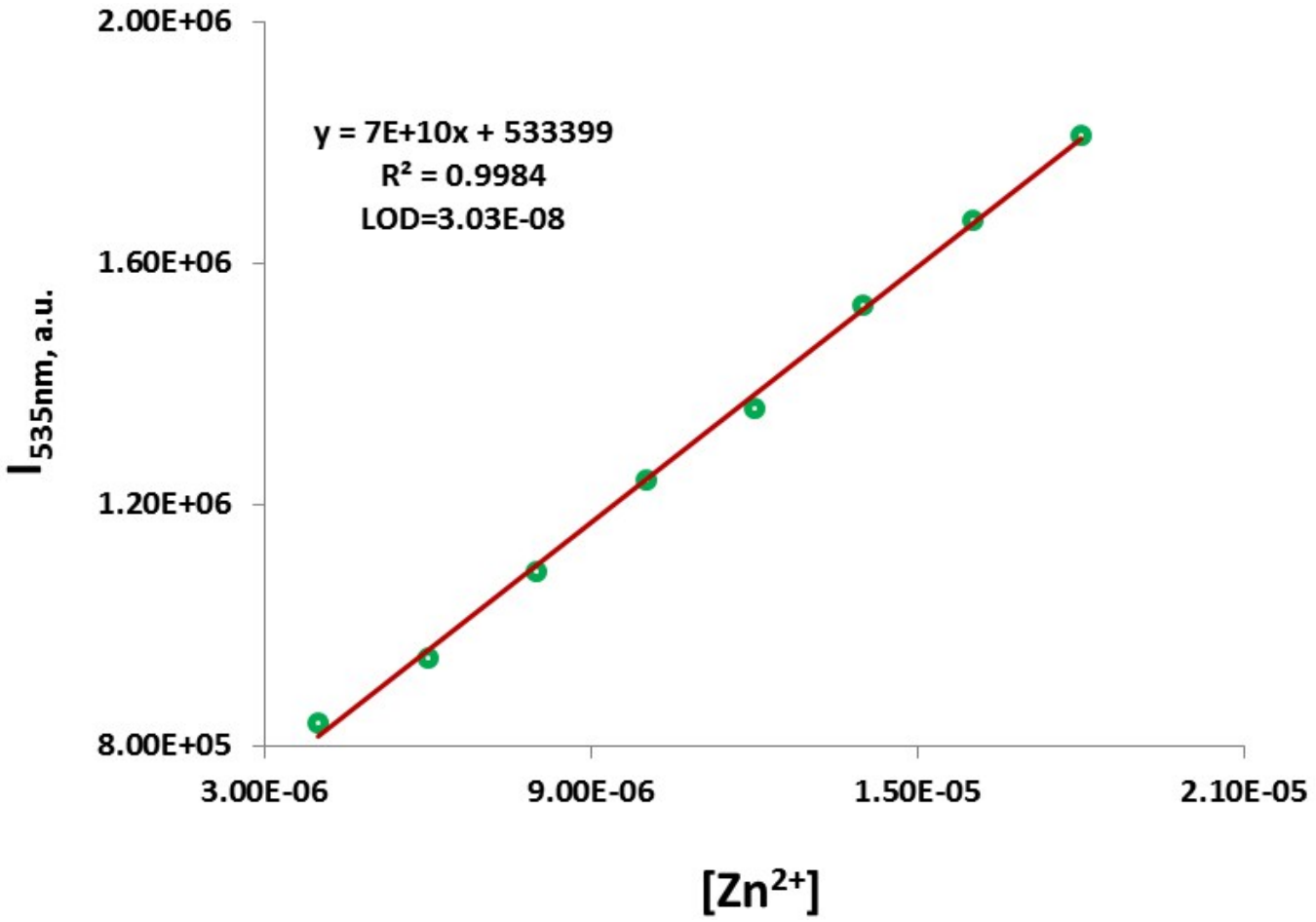

Figure S33: Mass spectrum of **CMD** after addition of Zn^{2+} (200 to 500 range)

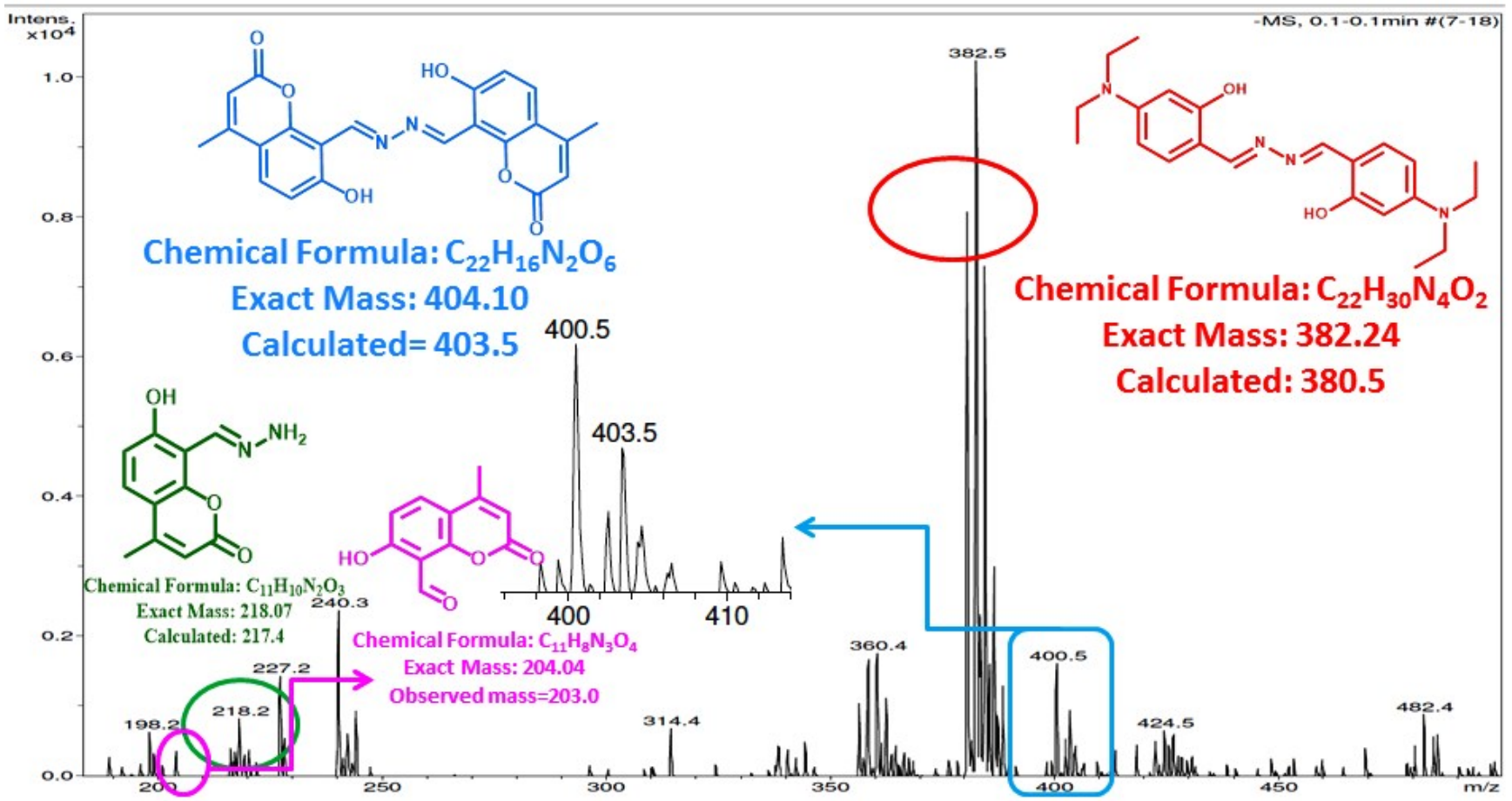

Figure S34: Mass spectrum of **CMD** after addition of Zn^{2+} (800 to 1500 range)

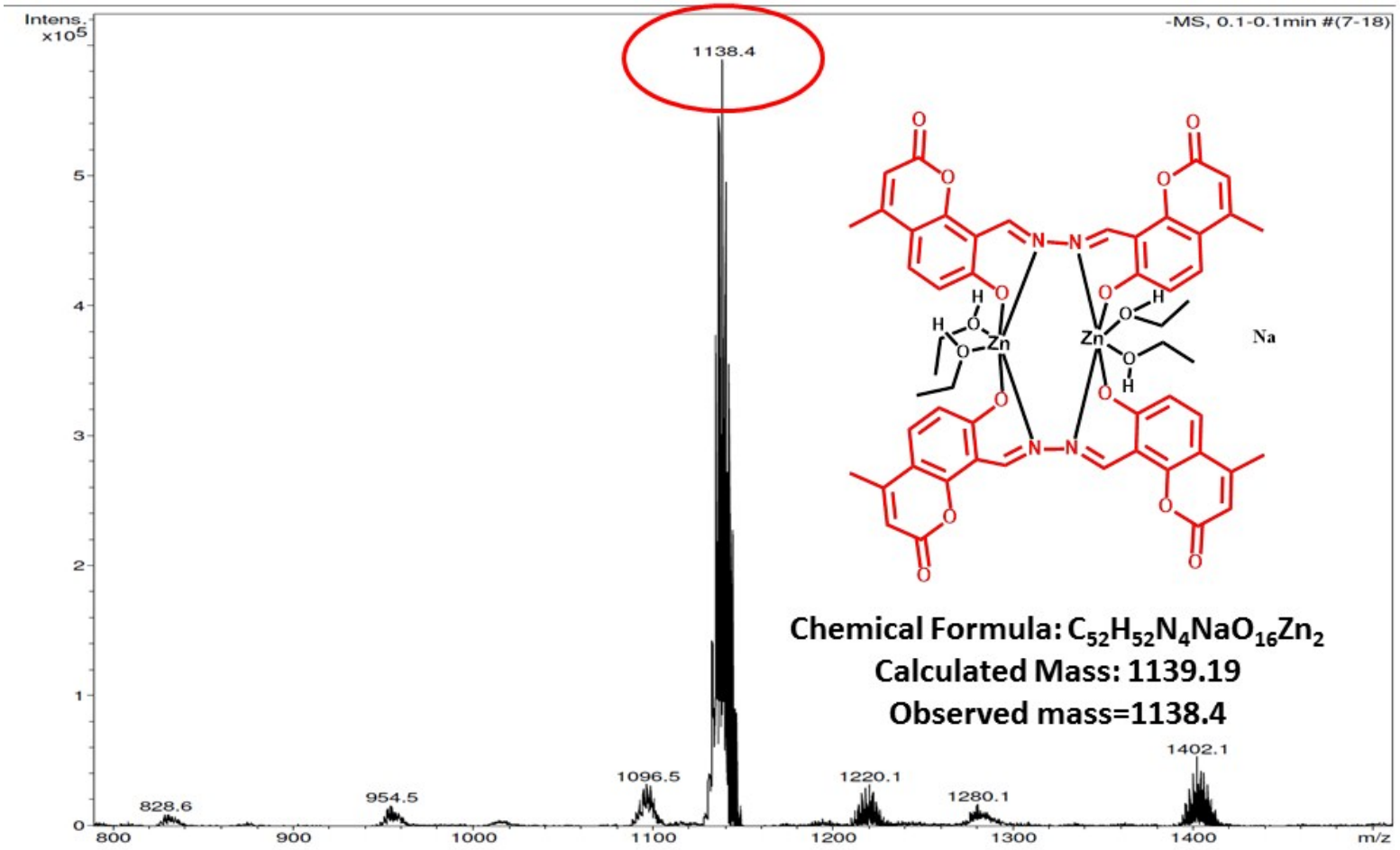

Fig. 35 Partial ^{1}H NMR spectra change with time upon addition of Zn^{2+} (10 equiv.) in **CMD** (DMSO-d_6) and the comparison of ^{1}H NMR peaks of resultant in-situ synthesized products with purely synthesized compounds CM, ACM-Hz and NSA.

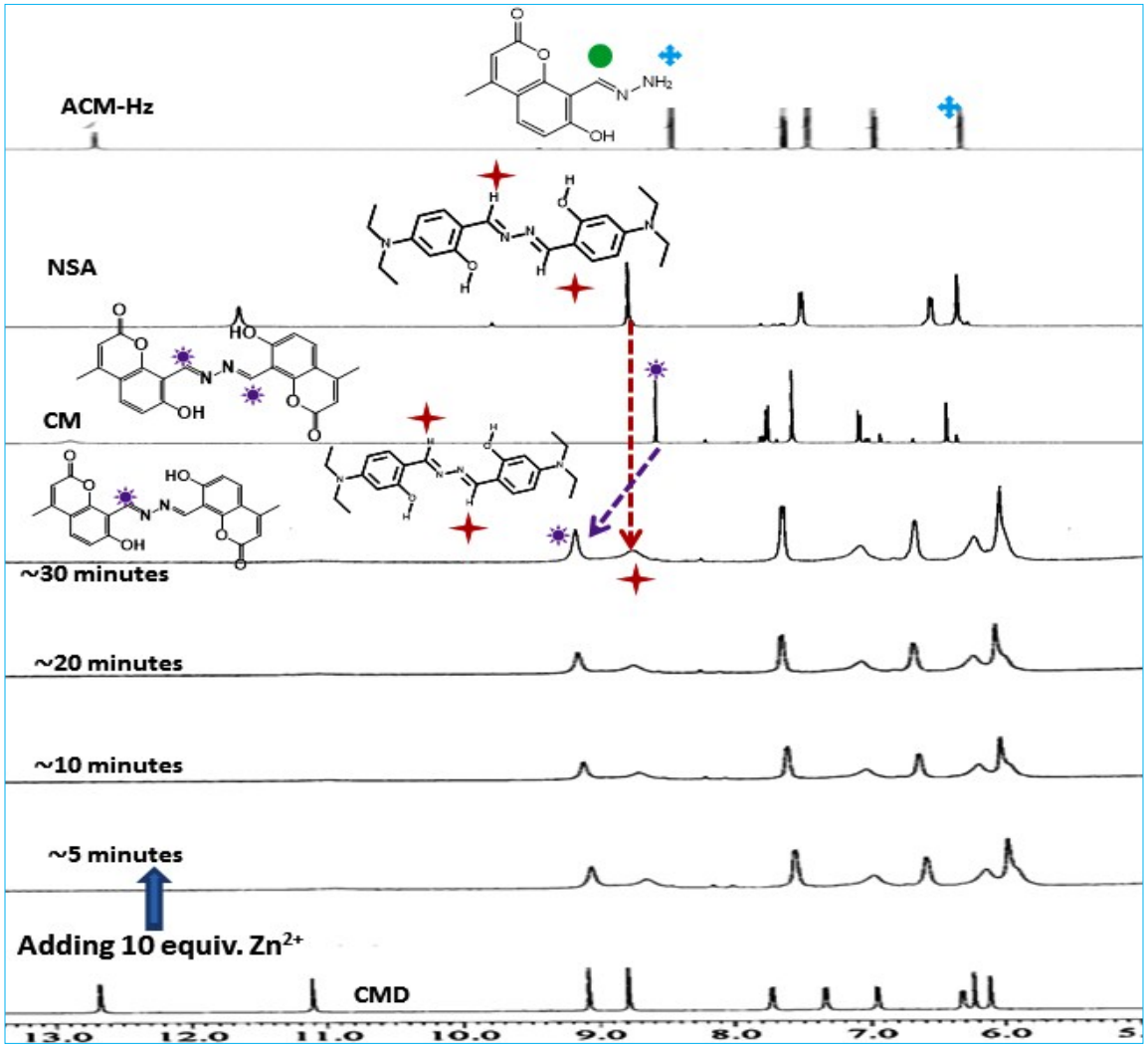

Figure S36 (a): (a) Emission spectra of **ACM, ACM-Hz, CMD, NSA** and **CM** with and without Zn^{2+}.**(b)** Emission spectra of **CM, CM-Zn-CM, CM-Zn-CM'+NSA** .

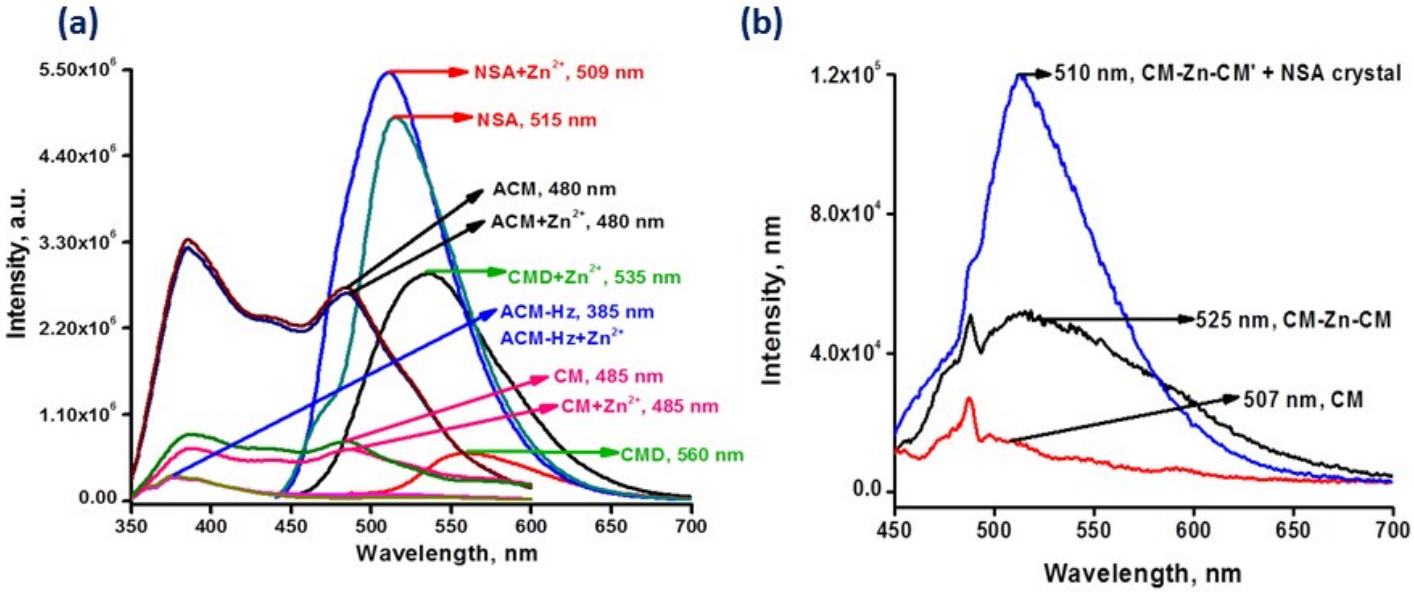

Figure S36 (b): Photograph showing fluorescence color change of **1(CMD), 2(CMD+Zn^{2+}), 3(CM), 4(CM+Zn^{2+}), 5(ACM-Hz), 6(ACM-Hz+Zn^{2+}), 7(NSA), 8(NSA+ Zn^{2+}), 9(ACM) and 10(ACM+Zn^{2+})** (under visible light) in presence of different metal ions in Ethanol.

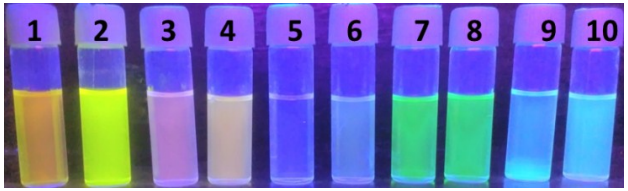

Figure S37: Absorption spectra of **CMD** and **NSA** with and without Zn^{2+}

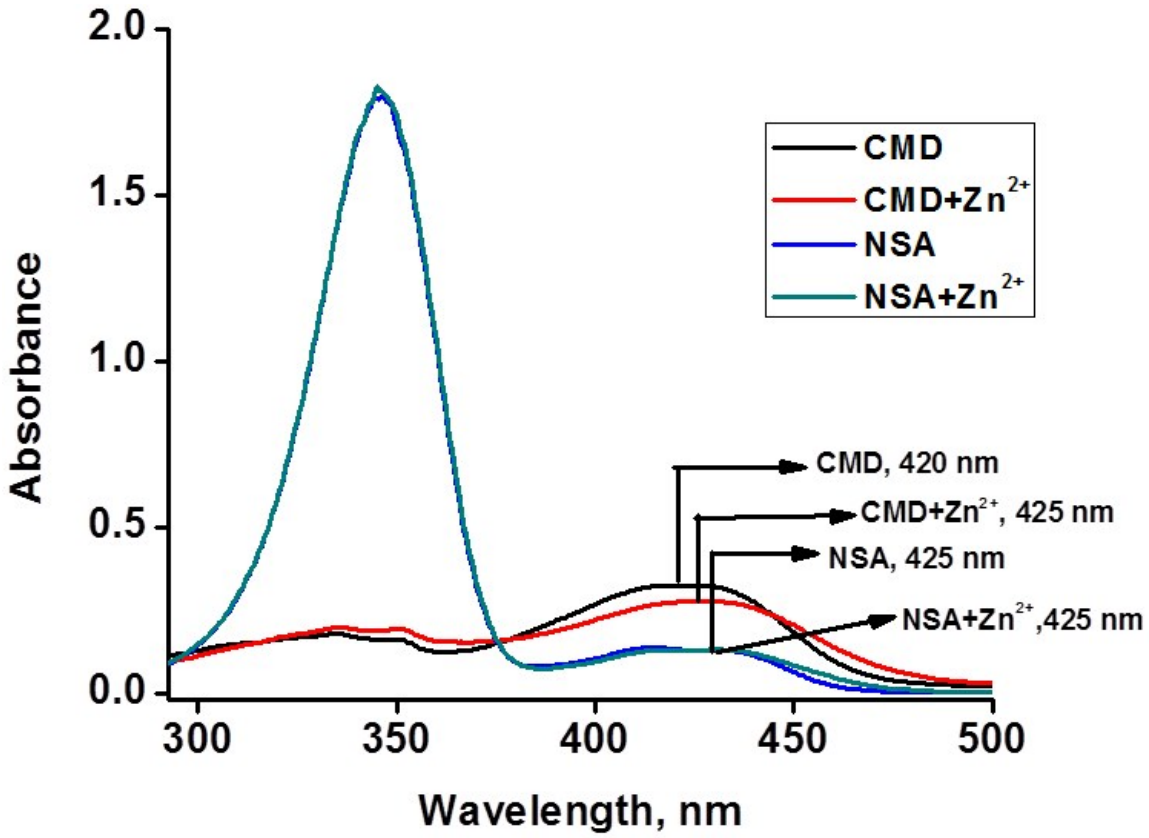

Figure 38: SEM image of **CMD** and **CMD+Zn^{2+}**.

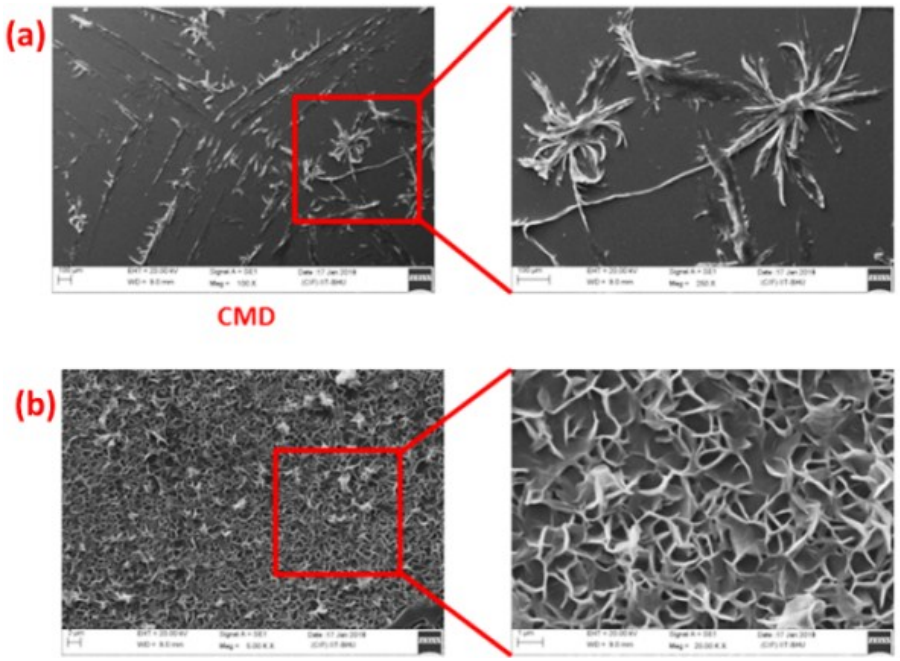

Figure S39: (a)Graph showed the percent cell viability of compound **CMD** measured through MTT assay at 24 h and of treatment of **CMD** and different concentration range of (2, 5, 10, 15, 20, 25, 30 µg/ ml media). Graph was plotted against

concentration (X- axis) to relative cell viability (Y-axis). (b)Graph showing the half maximal inhibitory concentration (IC50) range of the CMD and it was near the 25 µg and thus we exposed the cells within the range of IC50 value.